Cheng, Pengfei; Wang, Dong; Schaaf, Peter

A review on photothermal conversion of solar energy with nanomaterials and nanostructures: from fundamentals to applications

Original published in: Advanced sustainable systems. - Weinheim : Wiley-VCH. - 6 (2022), 9, art. 2200115, 19 pp.

Original published: 2022-07-06

ISSN: 2366-7486

DOI: 10.1002/adsu.202200115

[*Visited:* 2022-10-12]

ADVANCED SUSTAINABLE SYSTEMS
www.advsustainsys.com

A Review on Photothermal Conversion of Solar Energy with Nanomaterials and Nanostructures: From Fundamentals to Applications

Pengfei Cheng, Dong Wang,* and Peter Schaaf*

Solar energy is a green, sustainable, and de facto inexhaustible energy source for mankind. The conversion of solar energy into other forms of energy has attracted extensive research interest due to climate change and the energy crisis. Among all the solar energy conversion technologies, photothermal conversion of solar energy exhibits unique advantages when applied for water purification, desalination, high-temperature heterogeneous catalysis, anti-bacterial treatments, and deicing. In this review, the various photothermal conversion mechanisms based on different forms of heat release are summarized and some of the latest examples are presented. In addition, the necessary prerequisites for solar-driven photothermal materials toward their practical applications are also discussed. Further, the latest advances in photothermal conversion of solar energy are discussed, focusing on different types of photothermal applications. Finally, a summary is given and the challenges and opportunities in the photothermal conversion of solar energy are presented. This review aims to give a comprehensive understanding of emerging solar energy conversion technologies based on the photothermal effect, especially by using nanomaterials and nanostructures.

1. Introduction

In the coming era of "Carbon Peak and Carbon Neutrality,"[1,2] it is particularly important to develop new energy technologies with low cost, environmental friendliness, and industrial scale to replace the traditional fossil fuels,[2–6] which are widely considered to cause greenhouse effect and frequent extreme weathers. Solar energy is a kind of energy that never be worried about being run out and can be readily available for every country.[7,8] Therefore, it is the most promising alternative to fossil energy compared to nuclear energy,[9] wind energy,[10] and blue energy.[11] Among the solar energy conversion technologies,[12] silicon-based photovoltaic (PV) solar cell has been commercialized and the efficiency of monolithic silicon/perovskite solar cell has achieved over 29%.[13,14] Alternatively, photothermal conversion is another way to utilize solar energy and has drawn dramatically increasing attention due to the easily achievable large conversion efficiency (usually larger than 50%) for the applications in thermal catalysis,[15–18] water evaporation and desalination,[19–27] bacterial killing,[28] as well as thermal-responsive sensors.[29–31] Photothermal conversion of solar energy refer that solar energy is first converted into heat and then heat energy is utilized to achieve the desired destinations,[15,16,28,31–34] such as water purification, desalination, electric power generation, catalysis conversion, bacterial killing, and actuators. Thus, photothermal conversions of solar energy can be supplementary to PV-based technology in solar energy conversion and are deemed to be extremely important to clean energy production.[19,35,36]

Very recently, photothermal-derived applications have attracted many researchers' interests and great efforts have been taken to expand the application fields and increase the conversion efficiency based on solar energy conversion.[29,37–44] Among all the applications, photothermal water evaporation for desalination and water purification has attracted the most attention, owning that freshwater can be directly produced by only using solar energy and it can address the freshwater shortage challenge for many countries.[27,32,33,45–53] However, the research focusing on other applications has attracted less attention than photothermal water evaporation, which should also be taken equally important attention for making the most of solar energy. For example, photothermal catalysis for H_2 generation and CO_2 reduction can be applied to convert solar energy into chemical energy under high concentrated solar intensity, but the efforts are still far from enough. Although photothermal electric power generation can show a solar-to-electricity conversion efficiency exceeding 7% under 38 Sun,[54] its conversion efficiency remains very low under low concentration solar intensity, such as 1 Sun or ambient conditions. Thus, the trade-off between efficiency, costs, and practicality should be considered in future works. In addition, photothermal bacterial killing technology has proved that it can be efficiently used for killing bacteria under solar light illumination,[28] but whether it can be applied for human or animal wound treatment still needs to be discussed. Furthermore, solar energy can also cause thermally sensitive objects to reversibly change the physical properties for

P. Cheng, D. Wang, P. Schaaf
Chair Materials for Electrical Engineering and Electronics
Institute of Materials Science and Engineering and Institute of Micro and Nanotechnologies MacroNano
TU Ilmenau
Gustav-Kirchhoff-Str. 5, 98693 Ilmenau, Germany
E-mail: pengfei.cheng@tu-ilmenau.de; dong.wang@tu-ilmenau.de

The ORCID identification number(s) for the author(s) of this article can be found under https://doi.org/10.1002/adsu.202200115.

DOI: 10.1002/adsu.202200115

photothermal sensing.[29,55–57] Research on this application is also rare and more efforts should be paid in this area. Photothermal deicing technology is still in its infancy, because the related research only has been investigated in the laboratory and ignored practical operating conditions.[58–62] For example, icing risks will usually happen at car windows, power lines, and airplanes, and how to solve them under low temperature and poor solar intensity still need further investigation.

In this review, we mainly concentrate on the material types for photothermal conversion mechanisms, the necessary requirements for high-performance photothermal light absorbers and a series of photothermal applications based on solar energy conversion (**Figure 1**). First, four types of fundamental mechanisms of solar-driven photothermal conversion have been summarized, including non-radiative relaxation of semiconductors, plasmonic heating of metals, thermal vibrations of organic molecules and multiple interactions of micro/nanostructured materials. Besides, some complicated material systems will contain two or three combined basic mechanisms. Second, we discussed the essential requirements for high-performance solar-driven photothermal materials, such as excellent light trapping performance in broadband (especially in the whole solar spectrum), suitable heat conduction, low heat emission, and high multi-level stability (anti-corrosion, anti-bacterial, and anti-high temperature). Then, the state-of-the-art progress for photothermal conversions of solar energy is introduced in detail, mainly including photothermal water evaporation and desalination, photothermal catalysis, photothermal electric power generation, photothermal bacterial killing, photothermal sensors, and photothermal deicing. At last, we summarize the whole review and give the viewpoint on the opportunities and challenges faced by the future development of photothermal conversion based on solar energy and light absorbers. This review presents a broad scope of photothermal applications, offers a comprehensive understanding on the photothermal conversion of solar energy and provides a guideline for better design and fabrication of photothermal materials.

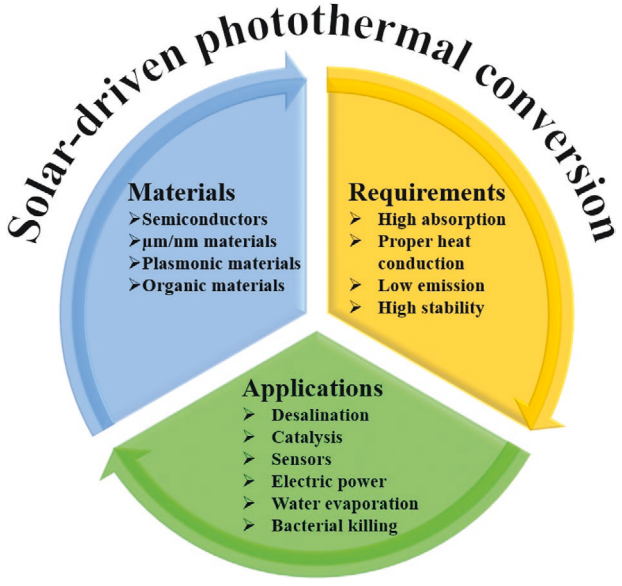

Figure 1. Schematic diagram of the scope of this review on solar-driven photothermal conversion.

2. Basic Mechanisms of Solar-Driven Photothermal Conversions

Conversion of solar energy into other forms of energy is urgently needed to address the global energy issues.[63,64] It can be realized by different conversion processes, such as PV effect,[4,65–67] photochemical transformation,[68–70] photoelectrochemical process,[71–73] photothermal conversion.[18,27,33] Among these processes, photothermal conversion is a straightforward way to harvest solar energy for solar storage and conversion,[27] which allows it to derive a series of applications, such as water evaporation and purification, desalination, electric power generation, bacteria-killing, catalysis, sensors, and so on. The photothermal effect, also the so-called photo-induced thermal effect, is produced by absorbing solar light and then releasing heat with the materials. These materials can be both organic materials (conjugated polymers, dyes, and macromolecules) and inorganic materials (such as carbon-based materials, semiconductors, and plasmonic metals). Based on different thermal release mechanisms of light interaction with matter, we classify these materials into four groups as shown in **Figure 2**:[24,27,33,74,75] 1) Non-radiative relaxation of semiconductors; 2) plasmonic heating of metals; 3) thermal vibration of organic molecules; 4) multiple interactions of micro/nanostructured materials.

2.1. Non-Radiative Relaxation of Semiconductors

Semiconducting materials convert solar energy into heat by absorbing the photon energy larger than their bandgaps, so that electrons in the valence band (VB) are able to be excited to the conductive band (CB). Next, excitation-state electrons and holes are produced in the CB and VB, respectively. Then, the excitation-state electrons and holes relax to the corresponding edges of CB and VB. As a result, the solar energy is successfully converted into heat, as shown in Figure 2a. However, radiative recombination of the excited carriers (electrons and holes) in direct bandgap will lead to photothermal performance loss by releasing photons. In addition, the reflection of light with a wavelength smaller than the band edge will also lead to low photothermal conversion efficiency. Usually, by heteroatom doping or vacancy concentration regulation, the cutoff wavelengths of semiconducting materials can move toward long wavelength (redshifts) and even till the optical bandgap disappear.

For example, crystalline silicon (c-Si) has been often used as a light absorber, because it has a suitable bandgap for solar energy harvesting. c-Si as a typical semiconductor has a bandgap of 1.12 eV, corresponding to a cutoff wavelength of 1110 nm. When it is used as a light absorber for photothermal conversion, only the energy beyond 1110 nm can be efficiently utilized. Cheng et al. reported that c-Si with high concentration boron atom doping and surface nanostructures can make the optical bandgap disappear, leading to the whole solar spectrum's absorption in the range from 300 to 2500 nm with high absorption of 98.9%.[34] In another case, TiO_2 as a typical wide bandgap material (≈3.2 eV) has a cutoff wavelength of 388 nm (ultraviolet light) and can only take advantage of a very limited range of solar energy. However, by introducing oxygen vacancies, the white TiO_2 powder changed into a black TiO_2

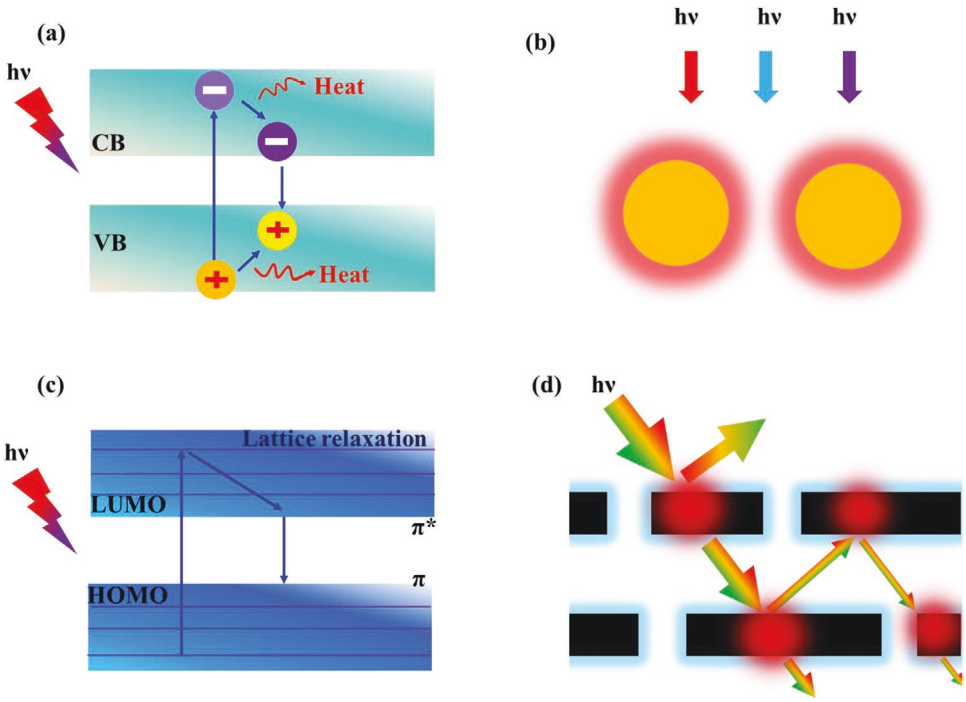

Figure 2. Solar-driven photothermal mechanisms of different light absorbers. a) The illustration for heat production from non-radiative relaxation in narrow bandgap semiconductors. b) The illustration for heat production from localized heat in plasmonic metals. c) The illustration for heat production from molecule vibrations in organic materials. d) The illustration for heat production from multiple interactions in micro/nanostructured materials.

one.[51,76–79] Accordingly, its cutoff wavelength is transferred from ultraviolet light into infrared light. As a result, the light absorption of oxygen-vacancy-rich TiO_2 is highly enhanced, which enables a wide range of applications.[80–82]

2.2. Plasmonic Heating of Metal Nanostructures

Metallic plasmonic nanoparticles, such as gold, silver, aluminum, and platinum nanoparticles, have a high concentration of free electrons within the metals.[26,27,52,83–85] When the collective oscillation of the free electrons is driven coherently by the oscillating electric field of light, the localized surface plasmon resonance (LSPR) phenomenon will occur on the surface of these metals, leading to enhanced radiative scattering of and absorption of resonant light. In addition, near-field enhancement and hot carrier generation can also result from the decay of the collective oscillations. All these depend on many factors such as particle size, form, composition, and dielectric environment.[86,87] The relaxation of the enhanced absorption in a non-radiative way by releasing thermal energy, is called the plasmonic photothermal effect. The exact mechanism of the plasmonic photothermal effect can be understood like that: the excited electrons at a higher energy level (hot electrons) have a limited lifetime and will release the absorbed energy through electron–electron and electron–phonon scatterings and then dissipate energy in the surroundings by phonon–phonon relaxation process.[26,27] During this process, solar energy is converted into heat (Figure 2b). Nanoparticles and nanostructures have a large cross section of absorption which allows the interaction with the light on a large scale, thus, metallic plasmonic nanoparticles with a strongly LSPR effect are promising candidates for solar energy conversion by the photothermal process.

Zhou et al,[88] reported a kind of gold plasmonic absorber fabricated by a physical vapor deposition method in a manner of self-assembly in an anodized aluminum oxide mask. The transparent AAO mask turns black and this plasmonic light absorber presents a light absorption of about 99% in the range from 400 nm to 10 µm, enabling strong photothermal conversion ability. As a result, the efficiency of solar steam generation exceeds 90% under 4 kW m^{-2} solar intensity using the gold plasmonic light absorber. However, gold is a kind of noble metal and it is expensive for solar steam generation. Considering this, Xu et al,[89] developed a cheaper nickel (Ni) nanostructure as the light absorber. The plasmonic light absorber can achieve absorption as high as ≈95% in the wavelength range from 200 to 1500 nm, which can be totally used for solar steam generation. By using the Ni plasmonic absorber for solar steam generation, the evaporation rate remarkably enhanced to ≈2.3 times compared with the control experiment.

2.3. Thermal Vibration of Organic Molecules

Some polymer materials and organic small molecule materials can efficiently convert photon energy into heat through lattice relaxation.[40,90–92] The mechanism of these kinds of organic materials is similar to that of semiconductors.[23,26,27] Such materials usually appear to be black or dark in color. In a typical photothermal conversion process (Figure 2c), The materials with abundant conjugated π bonds absorb the photon energy, and the electrons subsequently are excited from the ground state π orbit

(highest occupied molecular orbital, HOMO) to a higher excited π^* orbit (lowest unoccupied molecular orbital, LUMO). On one hand, heat will be released when excited electrons relax to the edge of LUMO energy level by lattice relaxation; on the other hand, when the incident photon energy matches a possible electron transition within the organic molecule, the excited electrons will come back to the HOMO energy level, leading to the heat release.

Chen et al,[92] designed a kind of organic-small-molecule photothermal material (CR-TPE-T) with strong π–π stacking in the solid state, which showed a broadband absorption in the wavelength range from 300 to 1600 nm. By lattice relaxation, the materials behaved with an excellent photothermal conversion efficiency of 72.7% under the intensity of 800 mW cm^{-1} using an 808 nm laser. In addition, integrating CR-TPE-T with porous polyurethane as a solar steam evaporator, it showed a high solar-to-vapor efficiency of 87.2% under 1 Sun intensity. Zhang et al,[93] developed polypropylene-polyethylene dioxythiophene-polypyrrole (PP-PEDOT-PPy) double-shell textile as a light absorber for solar and thermal energy harvesting. The flexible photo-thermoelectric device obtained a voltage of 536.47 μV under infrared light. This shows a potential for energy supply in smart wearable electronic devices.

2.4. Multiple Interactions of Micro/Nanostructured Materials

Micro/nanostructured materials include black carbon-based materials, black silicon, black GaAs, and other black materials.[21,31,34,52,53,94–99] Generally, bulk materials tend to have a limited emissivity. For example, a graphite sheet without micro/nanostructures has an emissivity of ≈0.85, which is not beneficial for solar energy harvesting.[26] Therefore, in order to improve light absorption of bulk materials, different micro/nanostructured materials, such as graphene, carbon nanotube, black silicon, and black GaAs nanostructures are put forward. The basic principle is to increase the times of reflections, refractions, and scatterings within the nanostructures, as presented in Figure 2d.[26,33] In this principle, incident photon energy is greatly trapped in the nanostructures and almost no photons are able to escape from them. Finally, the absorbed photon energy is released into the environment by heat radiation.

Ren et al,[21] developed a hierarchical graphene foam for highly efficient photothermal conversion. By reducing the reflection and transmission of the incident photons, the hierarchical graphene foam can achieve a high absorption for efficient solar-thermal energy conversion. While common graphene foam without hierarchical nanostructure shows a large portion of reflection and transmission, leading to a low absorption of incident light. When the hierarchical graphene foam is used for photothermal solar steam generation, it can obtain a maximum solar-thermal conversion efficiency as high as 93.4%. Wu et al,[61] reported a kind of superhydrophobic candle soot for photothermal deicing. The self-assembly hierarchical candle soot increased the optical path length and enabled the excellent light trapping property. Under 1 Sun irradiation for 5 min, the surface temperature of the hierarchical candle soot was increased to 53 °C, where no ice can exist above the environmental temperature of –50 °C. Cheng et al,[99] developed a 3D Ag hybrid plasmonic nanostructure for photo-thermoelectric conversion. The reported light absorber showed a maximum absorption >99% across the solar spectrum and the absorption ability was highly dependent on the structural height of the 3D structure, which verified that a high 3D structure would cause more times of reflections and thus gained a better light absorption performance. As a result, the high structure light absorber showed the best solar energy conversion performance.

2.5. Hybrid Mechanism of Other Materials

In order to meet the demand for practical applications, many hybrid materials with hybrid mechanisms have been developed. Generally speaking, hybrid mechanisms consist of two or two more fundamental mechanisms are mentioned above. For example, Huang et al,[90] developed one super-robust photothermal liquid metals@polymer core-shell material, which consists of plasmonic heating and thermal vibration of organic polymer mechanism during the heat production process. Zhang et al,[51] presented that the nanostructured silicon with gold nanoparticle deposition for photothermal conversion includes three fundamental mechanisms of non-radiative relaxation below the cutoff wavelength, plasmonic heating, and multiple interactions within the nanostructures in the wavelength range from 200 to 1700 nm. Li and his co-workers reported that Ti_3C_2 MXene with a characteristic absorption peak at ≈800 nm can show a nearly light-to-heat efficiency of 100%,[100] which possibly referred to plasmonic heating and multiple interactions within the nanostructures.[74]

3. The Fundamental Requirements for Solar-Driven Photothermal Materials

Solar-driven photothermal materials are promising platforms for addressing global energy challenges and environmental issues. Solar energy mainly focuses on the wavelength range from 300 to 2500 nm (**Figure 3**a), which occupies over 98% of solar energy. Therefore, as an excellent light absorber, it should achieve a high absorption in this range for solar energy conversion. At the same time, the reflection and transmission should approach zero. In addition, low heat emission is necessary to assure high photothermal conversion efficiency. Ultimately, suitable heat conduction will benefit heat transfer and boost photothermal conversion performance.

3.1. High Absorption with Broadband

High solar absorptance is the essential requirement and prerequisite. The solar absorptance can be defined as:[24,75,89]

$$A = \frac{\int_{\lambda_2}^{\lambda_2} (1 - R - T)\, S_{\text{solar}}\, \mathrm{d}\lambda}{\int_{\lambda_2}^{\lambda_2} S_{\text{solar}}\, \mathrm{d}\lambda} \quad (1)$$

where A, R, and T stand for absorptance, reflectance, and transmittance, respectively, S_{solar} is the wavelength-dependent

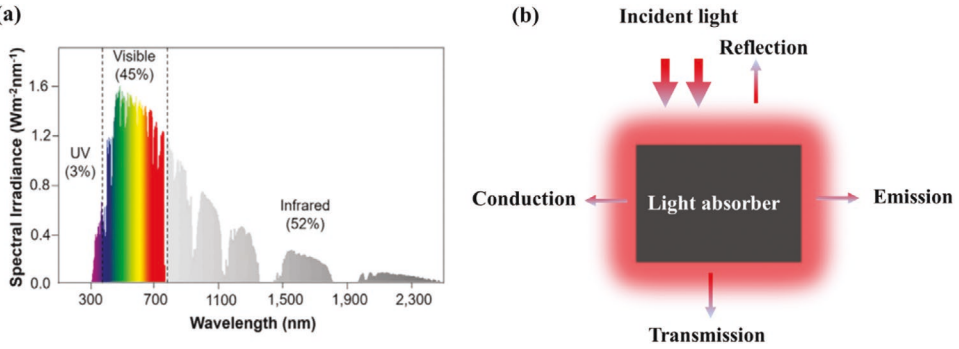

Figure 3. a) AM 1.5 G solar spectrum. Reproduced with permission.[33] Copyright 2019, Elsevier. b)The schematic illustration of heat generation, conduction, and emission processes with the light absorber.

AM 1.5 G solar spectrum, λ_1 and λ_2 are the integration beginning wavelength and end wavelength, respectively. According to this equation, by decreasing reflectance and transmittance, the solar absorptance can be enhanced. The maximum capability of photothermal conversion of one light absorber depends on its ability of the solar absorption. Therefore, it is necessary to apply different strategies based on different mechanisms to improve the solar absorptance of the broad band.[24,26] In this review, photothermal conversion is based on solar spectrum, thus the beginning wavelength λ_1 should be as small as possible, such as 300 nm, and the final wavelength usually is 2500 nm. In this range, solar energy can be efficiently absorbed by the light absorber.

3.2. Suitable Heat Conductivity of the Absorber

Suitable heat conduction of the light absorber is one of the key factors for directly photothermal conversion efficiency.[24,33,56] After the light absorber absorbs the solar light, the solar energy is transferred into heat by a photothermal process. The heat will be released mainly by heat conduction to a lower temperature object and heat radiation to the surrounding. The former directly decides the thermal transfer efficiency, while the latter will depend on the aims, for example, if the heat radiation is waste, the heat conductivity should be as small as possible. If the heat radiation is useful, the absorber should have a high conductivity to quickly release heat. The heat transfer of the light absorber can be defined as:[24,75]

$$q = kA\frac{(T_2 - T_1)}{L} \quad (2)$$

where q represents the amount of heat transfer by conduction, T_2 and T_1 are the steady temperatures of the light absorber and heat transfer object, respectively, k is the thermal conductivity of the light absorber, A is the area of the heat transfer, and L is the thickness of the light absorber. Thus, Equation (2) offers efficient paths to regulate heat transfer, such as picking up a suitable conductivity light absorber, enhancing heat transfer contact area, decreasing heat transfer thickness, and increasing the temperature differences ($T_2 - T_1$). For interfacial heating-based water evaporation and interfacial reaction, it is preferred to keep heat localized on the surface, and thus the heat conduction should be as low as much. For volumetric heating-based water evaporation and bacterial killing, heat should be transferred to the bulk water in time, so the heat conductivity should be high. In short, a reasonable thermal conductive material can be selected for photothermal applications according to desired purposes.

3.3. Low Emission of the Light Absorber

Low heat emission of the light absorber is another requirement for efficient photothermal conversion. It is well known that all objects will produce heat emission by releasing infrared electromagnetic waves. As is mentioned above, heat emission will cause heat loss and thus leading to lower solar energy conversion. In order to improve the solar energy conversion efficiency, the related thermal management technologies should be applied to reduce the heat loss, such as surface coating technology. Creating a lower emissivity surface layer on the light absorber while the light absorption performance is not affected, the solar energy conversion efficiency will be expected to be enhanced.

3.4. High Stability of Light Absorber

For the promising practical applications of photothermal-based technologies, high stability of the light absorber is also a necessary requirement,[33] in addition to the excellent broadband absorption, suitable thermal conduction, and low heat emission. The stability includes many aspects,[26,33] for example, 1) chemical stability: the chemical compositions will not be changed during the photothermal conversion process; 2) structure stability: the structure should keep stable during the long term cyclic temperature fluctuations with high resistance to light corrosion and/or solution corrosion; 3) optical stability: the reflection, transmission, and especially absorption should not be affected during the photothermal conversion processes.

4. Solar-Driven Photothermal Applications

4.1. Photothermal Water Evaporation and Desalination

Photothermal water evaporation has gained extensive attention because the readily available solar energy can be utilized to

treat different water sources (seawater, wastewater, and unpurified water) with highly efficient, environmentally friendly, and cost-effective to obtain fresh water, salts, and high energy water vapor for electric power generation.[26,45,81,82,92,97,101,102] For this type of application, the main challenges lay in finding suitable absorbers or absorber systems with high light absorption and fast heat transfer and water transport abilities to achieve high photothermal conversion efficiency, and a lot of theoretical and experimental studies have been concentrated on such issues.

In the past few years, photothermal water evaporation along with desalination has gone through huge advances based on water vapor production from liquid water with the assistance of solar light. The pioneering work of using a plasmonic absorber with strong light absorption for photothermal water evaporation was reported by Zhu's group.[32] The aluminum-based plasmonic absorber has three key features (**Figure 4**a,b): a) The porous anodic aluminum oxide (AAO) membrane works as the support and extends the optical path length for multiple reflections to improve absorption efficiency. b) Close-packed aluminum nanoparticles attached inside the AAO strongly interact with incident light for enhanced resonance absorption. c) A thin aluminum layer on the top of AAO can efficiently stop the light from penetrating the AAO membrane. These features make an aluminum-based plasmonic absorber achieve a light absorption as high as over 96% in the range from 400 to 2500 nm. The high efficiency and broadband absorption, strong LSPR, and efficient heat transfer lead to the high photothermal conversion efficiency of over 90% (Figure 4c) under 6 kW m^{-2} and a sharp decrease in salinity to meet the drinking water standard defined by World Health Organization (WHO). Similarly, Hu's group[103] reported that 3D mesoporous wood was decorated by metal nanoparticles to form plasmonic wood (Figure 4d). The plasmonic wood shows an outstanding light absorption performance (≈99%) in the range from 200 to 2500 nm (Figure 4e), which was caused by the LSPR effect of the metal nanoparticles and waveguide effect within the wood microchannels. The unique 3D mesoporous plasmonic wood with micro-nanochannels can effectively offer water transport channels and localized heat on the surface of metal nanoparticles. As a consequence, the 3D plasmonic wood can obtain a good photothermal conversion efficiency of 85% under 10 kW m^{-2} illumination (Figure 4f). It also showed an excellent stability for 6 days when applied for photothermal water evaporation. Different from the previous two works, Schaaf's group presented a 3D silver-based plasmonic absorber that was prepared on a glass substrate using the metastable atomic layer deposition combined with physical vapor deposition.[52] The optimized 3D silver-based plasmonic absorber exhibited a high absorption of 96.4% in the wavelength range from 200 to 2500 nm due to the strong LSPR effect of the silver nanoparticles and multiple scatterings within the nanostructures (Figure 4h). When it was applied for the bottom-heated-based water evaporation, the water evaporation rate was remarkably improved to 7.12 times under 1 kW m^{-2} compared with that without solar illumination (Figure 4i). These findings highlight that it is of great significance to integrate 3D nanostructures with metal nanoparticles

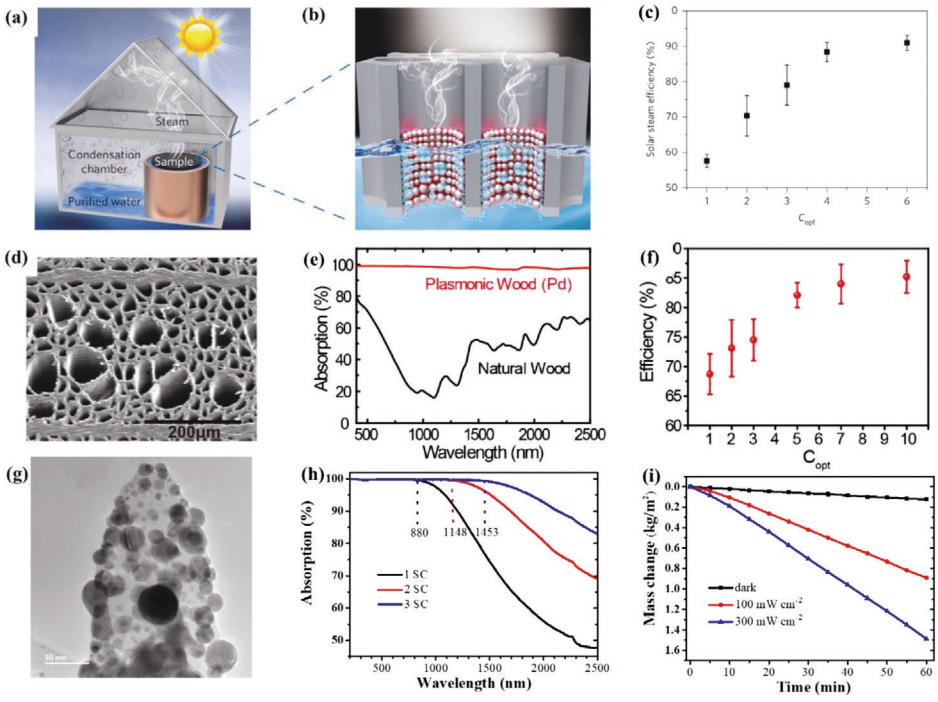

Figure 4. Photothermal water evaporation. a) The experimental set-up for photothermal desalination. b) Schematic illustration for water evaporation within the Al/AAO nanochannels. c) Photothermal water evaporation efficiency under different solar intensities. C_{opt} means optical concentration. (a–c) Reproduced with permission.[32] Copyright 2016, Springer Nature. d) Top-view SEM of plasmonic wood. e) Absorption spectrum of Pb plasmonic wood. f) Evaporation efficiency of Pa plasmonic wood under different solar intensities. (d–f) Reproduced with permission.[103] Copyright 2017, Wiley-VCH. g) TEM images of 3D Ag plasmonic absorber. h) Absorption spectrum of 3D Ag absorber under different conditions. i) Mass change curves with increasing time, which were used to calculate the efficiencies. (g–i) Reproduced with permission.[52] Copyright 2021, Elsevier.

to enhance solar energy harvesting and it also offers guidance for plasmonic light absorbers design when it is used for photothermal water evaporation.

4.2. Photothermal Catalysis

Photothermal catalysis can be usually understood as occurrence or acceleration of the catalytic reaction by the support of photothermal effect. The catalyst systems can be also used as photothermal conversion agent to increase the reaction temperature by converting solar energy to thermal energy, so that the reaction can be activated or reaction kinetics can be accelerated just like the situation in thermocatalysis.[15,16,75,104–106] In addition to the photothermal effect, some semiconducting and plasmonic catalysts also possess a synergetic effect of generated charge carriers by photon excitation, for example excited electrons and holes with semiconductors and hot electrons with plasmonic nanostructures, which sometime even plays the dominant role for the improvement of catalytic performance.[106,107] Nowadays, it is a new trend to develop new catalyst systems by rational design and taking the advantage of the synergy between both photothermal effect and generated charge carrier effect.[106–108] These processes are different from the photo-electrocatalysis process, which mainly depends on efficiently photogenerated electron–hole separation for promoting chemical reactions. This is also distinct from thermal catalysis, which tends to occur at a high temperature without solar illumination and the chemical reactions was driven by temperature.[18,109] During the photothermal catalysis process, solar energy can be used to destroy the chemical bonds to degrade organic pollutants. At the same time, it also can generate new chemical bonds for energy storage in hydrogen (H_2),[16] carbon oxide (CO),[35] methane (CH_4),[110] and so on. Therefore, photothermal catalysis can be an alternative or complementary method to thermal catalysis and photo-electrocatalysis, and provide an effective and promising path for addressing energy crisis and environmental problems.

4.2.1. Photothermal Catalysis for H_2 Generation

H_2, as a clean energy source, is promised to reduce environmental issues due to no pollution gas emission and "green house" gas emission during its usage process. Photothermal catalysis for H_2 production is an effective method to produce H_2 using solar light and suitable catalysts. Sourav Rej et al.[111] reported that TiN-Pt nanohybrids included a TiN core and multiple Pt nanocrystals attached to the TiN surface (**Figure 5**a), which can be used as a catalyst for H_2 production under the solar light based on a synergistic effect from both plasmonic hot electrons and photothermal heating.[113] It is noted that an apparent quantum yield of hot electron-caused H_2 production from NH_3BH_3 can achieve 120% under the resonant wavelength at 700 nm (Figure 5b). Experimental results (Figure 5c) indicated that the synergistic effect of hot electrons and collective-heating contribution can enhance the activity of TiN-Pt nanohybrid up to ≈11 times under 10 kW m^{-2} than under dark condition.

Huang and his colleague[44] also reported the low-temperature H_2 evolution from NH_3BH_3 via photothermal dehydrogenation. They prepared Ti_2O_3 nanoparticles (Figure 5d) as the photothermal catalyst by reducing TiO_2 nanoparticles using CaH_2. By introducing oxygen vacancies, the Ti_2O_3 totally turned black, allowing a broadband absorption in the whole solar spectrum (Figure 5e). As-prepared black Ti_2O_3 nanoparticles showed good chemical stability and narrow bandgap and also exhibited a fast H_2 generation from NH_3BH_3 at ambient temperature. Furthermore, when $CuCl_2$ was applied as the promoter, the H_2 production yield under 1 kW m^{-2} at 70 °C could achieve the same level under 9 kW m^{-2} (Figure 5f), indicating that it can be potentially used in hydrogen energy vehicles based on the related fuel cell technologies. However, current works only concentrate on one application for H_2 production.

In order to enhance the solar energy conversion efficiency, Gao et al.[112] presented a novel photothermal catalytic (PTC) gel for both freshwater and hydrogen generation. The PTC gel was prepared by decorating TiO_2/Ag nanofibers into chitosan with special freezing technology and freezing-drying. The reported 3D PTC gel (Figure 5g) has a hydrophobic interface to ensure fresh water and H_2 cogeneration. The 3D PTC gel showed a broadband absorption larger than 90% in the range from 250 to 2500 nm (Figure 5h). Its PTC H_2 production rate was remarkably enhanced under the full solar spectrum than under the solely UV light due to the obvious PTC effect. Furthermore, the PTC gel showed a good H_2 production stability (Figure 5i). In addition, the PTC gel can achieve a freshwater yield of up to about 5 kg m^{-2} under natural solar light illumination in 1 day. In short, integrating broadband light absorbers with co-catalysts can greatly enhance the H_2 yield based on photothermal catalysis using solar energy. Besides, developing multi-functional light absorbers is highly demanded for promoting solar energy conversion efficiency.

4.2.2. Photothermal Catalysis for CO_2 Reduction

Owning to increasing global fossil fuel consumption, CO_2 concentration in the air has been rising during the past years, leading to a series of environmental problems, such as global warming and extreme weather.[63,117] Photothermal catalysis for CO_2 reduction based on solar energy is one of the most promising strategies to tackle these issues. Most recently, Cai and his colleagues[114] reported a supra-photothermal catalyst nanostructure inspired by the "greenhouse" effect. The prepared photothermal catalyst showed an excellent CO_2 reduction performance compared with traditional ones. The catalyst (**Figure 6**a) included several nickel nanocrystals wrapped by a porous silica (Ni@p-SiO_2), which was thought to be beneficial for CO_2 reduction. Under the 2.8 W cm^{-2} illumination, the Ni@p-SiO_2 can exhibit the best photothermal performance than the other two catalysts (Figure 6b). In addition, the local temperature of Ni@p-SiO_2 was also the highest than those of Ni-based ones without SiO_2 shell. The authors believed that the excellent heat insulation and infrared shielding effect of silica resulted in the supra-photothermal CO_2 reduction performance. As a result, the Ni@p-SiO_2 photothermal catalyst can achieve a CO_2 conversion rate as high as 0.344 mol g^{-1} min^{-1}

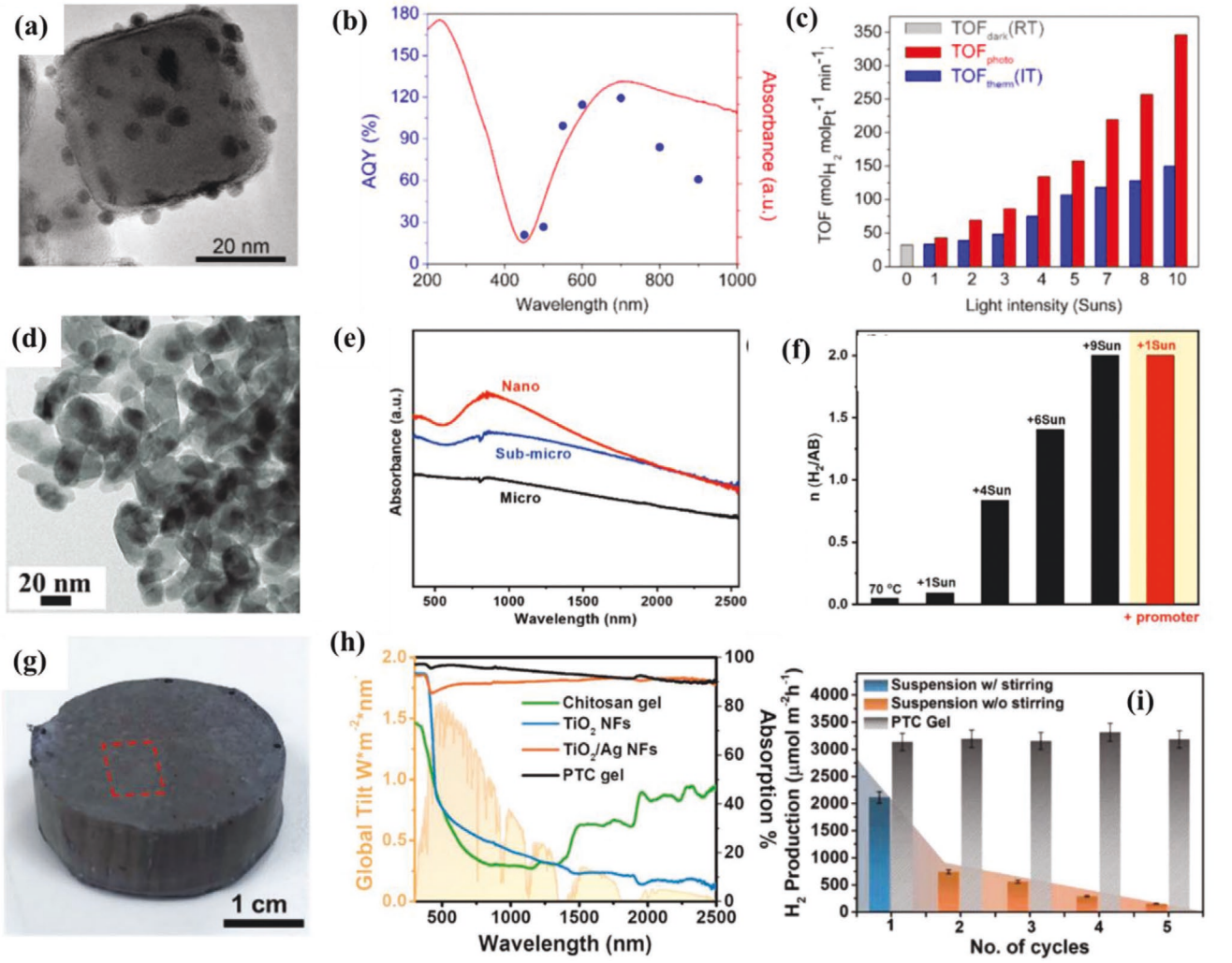

Figure 5. Photothermal catalysis for H_2 generation. a) TEM image of TiN–Pt photothermal catalyst. b) Absorption spectrum of TiN–Pt and corresponding apparent quantum yield (AQY). c) H_2 production rate under different solar intensities. (a–c) Reproduced with permission.[111] Copyright 2020, American Chemical Society. d) TEM image of Ti_2O_3 nanoparticles. e) Absorption spectrum of Ti_2O_3 particles with different scales. (d–f) Reproduced with permission.[44] Copyright 2020, Wiley-VCH. f) Hydrogen generation under different conditions using Ti_2O_3 nanoparticles. g) Optical photo of PTC gel catalyst. h) Absorption spectrum of the different samples. i) Hydrogen generation rate of suspension system with or without stirring. (g–i) Reproduced with permission.[112] Copyright 2020, Wiley-VCH.

under 2.8 W cm^{-2} illumination (Figure 6c). Besides, it also performed good stability for ten cycles and had an excellent CO selectivity as high as 90%.

Song et al.[115] showed a series of Fe-based photothermal catalysts (Fe, Fe_3C, Fe_3O_4, C@Fe_3C, and Fe@Fe_3C) prepared by a facile reduction reaction and carbonization treatment with Fe_3O_4 as the precursor. Figure 6d is the representative high-resolution TEM picture of Fe_3C. Under the 2.05 W cm^{-2} illumination, the surface temperature of Fe_3C gradually raised to 310 °C after half an hour, while Fe_3O_4 could achieve 350 °C within the same period (Figure 6e). Interestingly, during the photothermal catalysis for 12 h, Fe_3O_4 showed almost 100% selectivity for CO generation in the whole period, while the selectivity for hydrocarbons generation of Fe_3C was gradually increased from ≈38% to nearly 97.5% (Figure 6f). Meantime, it also presented that the selectivity could be regulated by adjusting the contents of the precursor during the treatment process.

Zhang et al.[116] reported a kind of silicon nanowire array with cobalt as the catalyst and silica as the coating (SNA@Co@SiO_2, Figure 6g) for photothermal CO_2 catalysis with almost 100% absorption in the whole solar spectrum. Figure 6h is the time-dependent temperature curves of different Si-based samples. Obviously, SNAs@$Co_{5\ min}$ demonstrated the best photothermal conversion performance and achieve the biggest surface temperature of 250 °C under 25 kW m^{-2} illumination. By controlling the sputtering time of Co, the photothermal performance of SNAs@$Co_{5\ min}$ was further optimized to SNAs@$Co_{15\ min}$ (Figure 6i). However, the stability of SNAs@$Co_{15\ min}$ was still unsatisfactory. To further improve the stability, silica was coated on the catalyst. Experimental results indicated that the stability of SNA@Co@SiO_2 was enhanced while the selectivity for CO production was a little decreased.

Fu and co-workers[110] reported almost 100% selectivity for CO_2 reduction to CH_4 was achieved using broadband

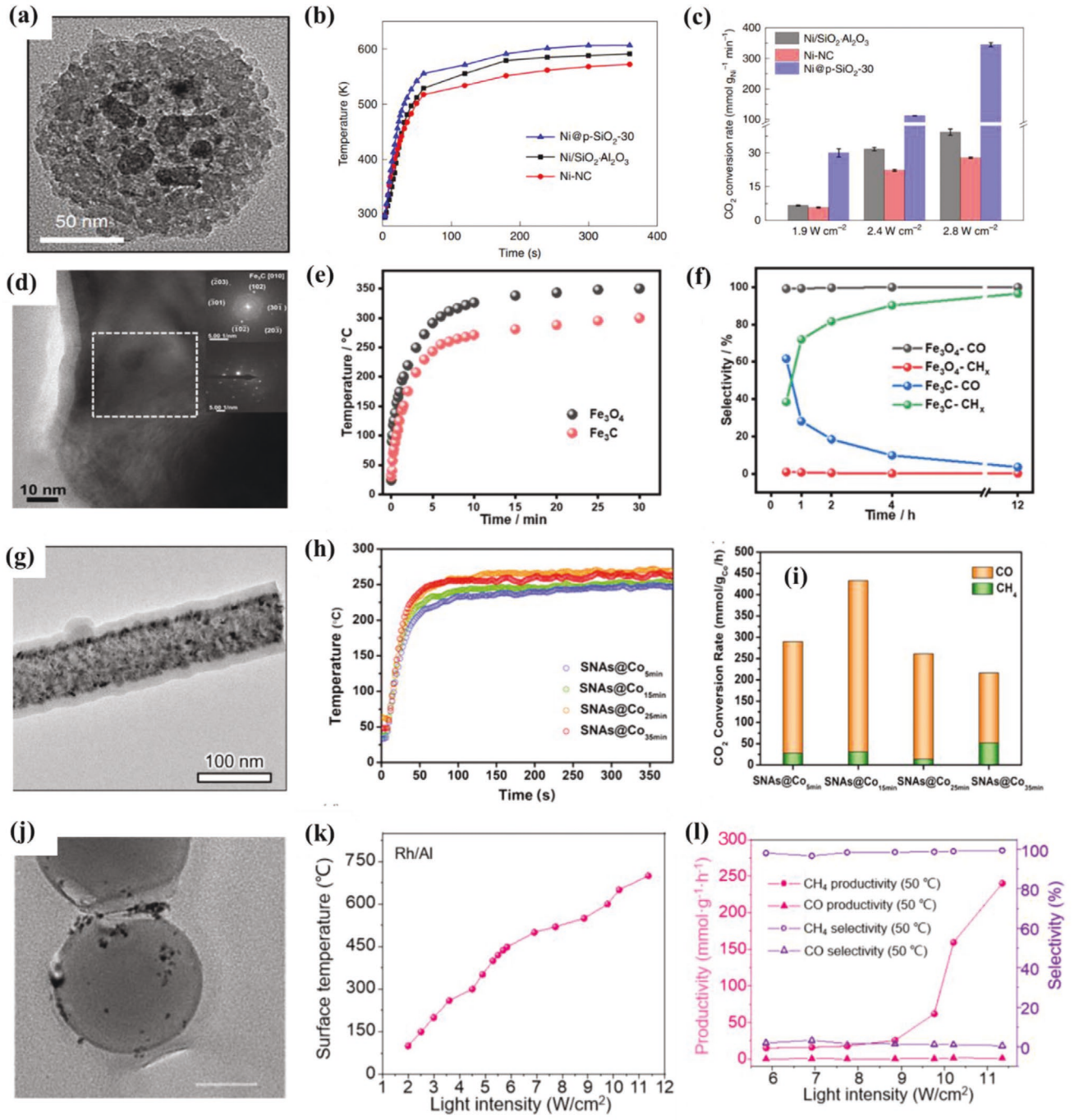

Figure 6. Photothermal catalysis for CO_2 reduction. a) TEM image of Ni@p-SiO_2-30. b) Photothermal performances of Ni@p-SiO_2-30, Ni@SiO_2-Al_2O_3, and Ni NCs. c) CO_2 conversion rates under different solar intensities. (a–c) Reproduced with permission.[114] Copyright 2021, Springer Nature. d) TEM image of Fe_3C nanocrystal. e) Photothermal performances of Fe_3C and Fe_3O_4. f) Selectively catalyze CO_2 to CO or CH of Fe_3C and Fe_3O_4. (d–f) Reproduced with permission.[115] Copyright 2020, American Chemical Society. g) TEM image of SNAs@$Co_{15\ min}$@SiO_2. h) Photothermal performances of SNAs@$Co_{15\ min}$, SNAs@$Co_{25\ min}$, SNAs@$Co_{35\ min}$, and SNAs@$Co_{45\ min}$. i) CO_2 conversion rates under different photothermal catalysts. (g–i) Reproduced with permission.[116] Copyright 2021, Wiley-VCH. j) TEM image of the Rh/Al nanoantenna catalyst. k) Photothermal performances of Rh/Al nanoantenna catalyst under different solar intensities. l) CO and CH_4 production rates under different solar intensities and their corresponding selectivity. (j–l) Reproduced with permission.[110] Copyright 2021, American Chemical Society.

Rh/Al nanoantenna photothermal catalyst and high-concentrated solar energy. The catalyst was prepared by a simple solvothermal method and the structure of Rh/Al can be seen in Figure 6j, where ultrafine Rh nanoclusters with several nanometers adhered on the Al nanosphere. Figure 6k exhibits the sample surface temperature was changed by the solar intensity and the highest temperature could reach ≈700 °C at the solar intensity of 11.3 W cm^{-2}. Figure 6l demonstrates that

photothermal catalysis CO_2 methanation could show almost 100% selectivity under different solar intensities at 50 °C. These research results offer the idea concept that rational design of broadband photothermal catalyst is beneficial for CO_2-to-fuel conversion.

4.3. Photothermal Electric Power Generation

Apart from PV electric power generation,[12,67] electric power could also be produced through the photo-thermoelectric effect in which solar energy is utilized by combining light absorber and thermoelectric modules. Generally, a photo-thermoelectric conversion process includes that: 1) the light absorber absorbs the solar light and converts it into heat, resulting in a high temperature surface on the light absorber; 2) the back side of thermoelectric modules is against the solar light and it will achieve a low surface temperature; 3) the temperature difference (ΔT) between the high temperature and low temperature will form a driving force and the force will drive thermoelectric modules to generate electricity.

Photo-thermoelectric power generation technology can be widely applied in wearable electronics and micro-electronic chips due to low voltage and small electricity outputs. Ho's group reported a flexible and thermal insulative organic light absorber sponge for electric power and water vapor cogeneration. The sponge consisted of carbon nanotubes/cellulose nanocrystal coating and a porous polymer support. **Figure 7**a presents the SEM picture of the light absorber and the inset was the optical image. Obviously, its appearance was totally

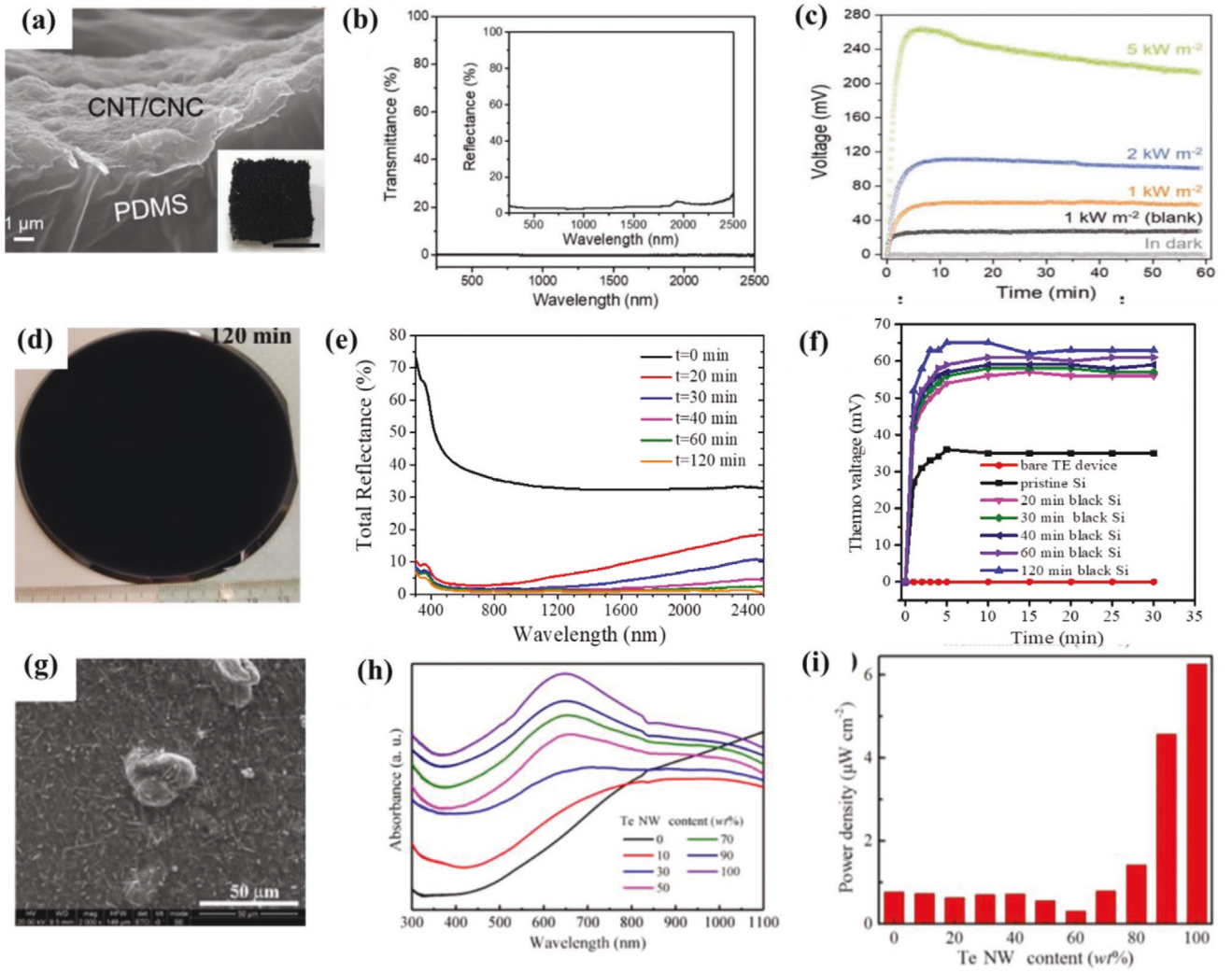

Figure 7. Photothermal electric power generation. a) SEM image of CNT/CNC@PDMS sponge and the inset is the digital photo (scale bar: 1 cm). b) light trapping performance of CNT/CNC@PDMS sponge. c) Photo-thermoelectric conversion results under different solar intensities. (a–c) Reproduced with permission.[39] Copyright 2019, Wiley-VCH. d) Optical photo of black silicon with 120 min etching time. e) Light trapping performance of black silicon with 120 min etching time. f) Photo-thermoelectric conversion results with different samples under different solar intensities. (d–f) Reproduced with permission.[34] Copyright 2021, American Chemical Society. g) SEM image of PEDOT:PSS/Te NW (90 wt% Te NWs) films. h) Absorption performance of different Te NW content of PEDOT:PSS/Te NW films. i) Photo-thermoelectric conversion results for different Te NW content of PEDOT:PSS/Te NW films. (g–i) Reproduced with permission.[118] Copyright 2021, American Chemical Society.

dark, leading to a high light trapping performance (Figure 7b). Under the different solar intensities (Figure 7c), the thermovoltage output gradually increased and the maximum steady voltage (≈240 mV under 5 kW m^{-2} illumination) was high enough to power a calculator. But under the real environment (1 kW m^{-2}, AM 1.5 G), the steady voltage was only about 50 mV, which was unsatisfactory for many practical usages.

Cheng et al.[34] prepared an ultra-black silicon nanostructure (Figure 7d) with excellent light absorption property for high-performance photo-thermoelectric conversion. The optimized black silicon exhibited a super low reflection (Figure 7e). When the black silicon light absorber was assembled with thermoelectric modules for photo-thermoelectric generation, it could achieve a steady voltage of ≈64 mV (Figure 7f) under AM 1.5 G illumination, which showed a performance rise rate of 28% compared with the former work. To further simplify the photo-thermoelectric device, Liu and his colleagues[118] integrated the light absorber with thermoelectric material into one device for photo-thermoelectric power generation. As-prepared poly (3,4-ethylenedioxythiophene): poly(styrenesulfonate)/Te nanowires (PEDOT: PSS/Te NW) can be seen in Figure 7g. The sample with 100% Te concentration showed a highest broadband absorption in the 300–1100 nm (Figure 7h) and also a highest power density of ≈6 μW cm^{-2} (Figure 7i). To conclude, photo-thermoelectric power is a promising solar energy conversion technology, but many efforts should be made to improve the solar-to-electricity efficiency, because the efficiency remains still very low based on photo-thermoelectric conversion under AM 1.5 G illumination.[34,90,91]

4.4. Photothermal Bacterial Killing

Photothermal bacterial killing is distinct from photocatalytic bacterial killing,[7,119] which uses photo-induced strong oxidation groups to destroy the cell membrane for killing bacteria to death. It is based on chemical reactions and can be cataloged as a chemical method. Photothermal bacterial killing is referred that the protein of the bacterial is destroyed when it suffers from a high temperature under solar illumination, which is based on a physical method.[119] Therefore, the photothermal bacterial killing can be an efficient water treatment for improving water quality to decrease health risks and also can provide a reference for photothermal cancer therapy.

Photothermal bacterial killing as a highly efficient, green, and sustainable technology has been extensively studied due to its great importance for human health. Here, we choose the three-representative works as the indicators. In the year 2019, Pan et al.[120] reported a cost-effective and stable photothermal membrane for photothermal anti-bacterial application. By adjusting the precursor $(NH_4)_2S_2O_8$ concentration, the samples' surface gradually turned totally black (**Figure 8**a). The light trapping performance was thus increased and the reflection can be reduced to below 5% in the whole range from 200 to 1500 nm (Figure 8b). When the photothermal membrane was employed for bacterial killing under 4.5 kW m^{-2} illumination, the bacterial concentration remarkably decreased to a safe value and it could not be observed anymore by the naked eyes after culture (Figure 8c), which was thought to be almost no threat to mankind health.

Zhao et al.[121] demonstrated a $Co_{2.67}S_4$-based photothermal membrane that could be applied for photothermal anti-bacterial and water evaporation simultaneously. The $Co_{2.67}S_4$ nanoparticles (Figure 8d) and $Co_{2.67}S_4$-based photothermal membrane were prepared through the facile solvothermal method and vacuum-filtration method, respectively. The prepared $Co_{2.67}S_4$-based photothermal membrane exhibited a high absorption of ≈95% in the 200–2500 nm region (Figure 8e). To examine the photothermal anti-bacterial performance of the $Co_{2.67}S_4$-based membrane, a kind of *Escherichia coli* widely existed in wastewater was used as the model. As shown in Figure 8f, the Final-PTFE ($Co_{2.67}S_4$-based) membrane with light irradiation could cause all *E. coli* death while the sample without photothermal membrane didn't influence the *E. coli* growth. In addition, the $Co_{2.67}S_4$-based photothermal membrane could also achieve a photothermal conversion efficiency of 82% for water evaporation under 2 kW m^{-2} radiation. One step further, Qu et al.[41] reported a more effective Au/Ti_3C_2 photothermal membrane with a higher photothermal water evaporation efficiency of 83.6% and a faster sterilization rate. By exfoliating Ti_2C_3 from Ti_2AlC_3, followed by reduction Au on Ti_2C_3 and vacuum-filtration, Au/Ti_2C_3 photothermal membrane (Figure 8g) was prepared. It showed a broadband absorption in the 200–2500 nm region (Figure 8h). When applied as the photothermal membrane, it can lead bacterial death to about 7 orders of magnitude decrease in 10 or 20 min (Figure 8i). Furthermore, the stability of the Au/Ti_2C_3 photothermal membrane can remain pretty good during water evaporation. Above all, these researches provide the direction toward developing multifunctional, broadband, stable, and low-cost photothermal materials to improve the water quality by effectively harvesting solar energy in future.

4.5. Photothermal Sensors

Different from above-mentioned applications, photothermal sensors are referred devices that the physical property such as electrical resistance changes induced by the photothermal effect.[29–31] Usually, the thermistor is a kind of temperature sensor based on the thermal-sensitive resistor. When it is integrated with a light absorber, and placed under the solar light, the light-caused heat will influence its resistance, which can be easily measured according to the changed electric signals. In addition, photothermal actuators can be also constructed,[55,122] to convert solar energy into motion energy.

Besides, Xiang et al.[30] presented a series of cost-effective short-wave infrared sensors (**Figure 9**a) prepared by wet-method colloidal gold nanorods. The response wavelength ranges of these sensors are from 900 to 1300 nm (Figure 9b). Under the illuminations, the assembled hybrid gold nanorods @ thermistor (Figure 9c) showed a remarkable photo-induced resistance drop, reflecting the electric signal change in Figure 9c. However, it only referred to a narrow band response.[77–79] To address this challenge, Xiong and her colleagues[29] presented a broadband photodetector (Figure 9d) that integrated a reduced graphene oxide (rGO) layer with a thermistor. By wrapping rGO film onto a polydimethylsiloxane (PDMS) layer, the sample exhibited a broadband light absorption in 200–1300 nm (Figure 9e), resulting in an excellent photothermal performance. Under 0.8

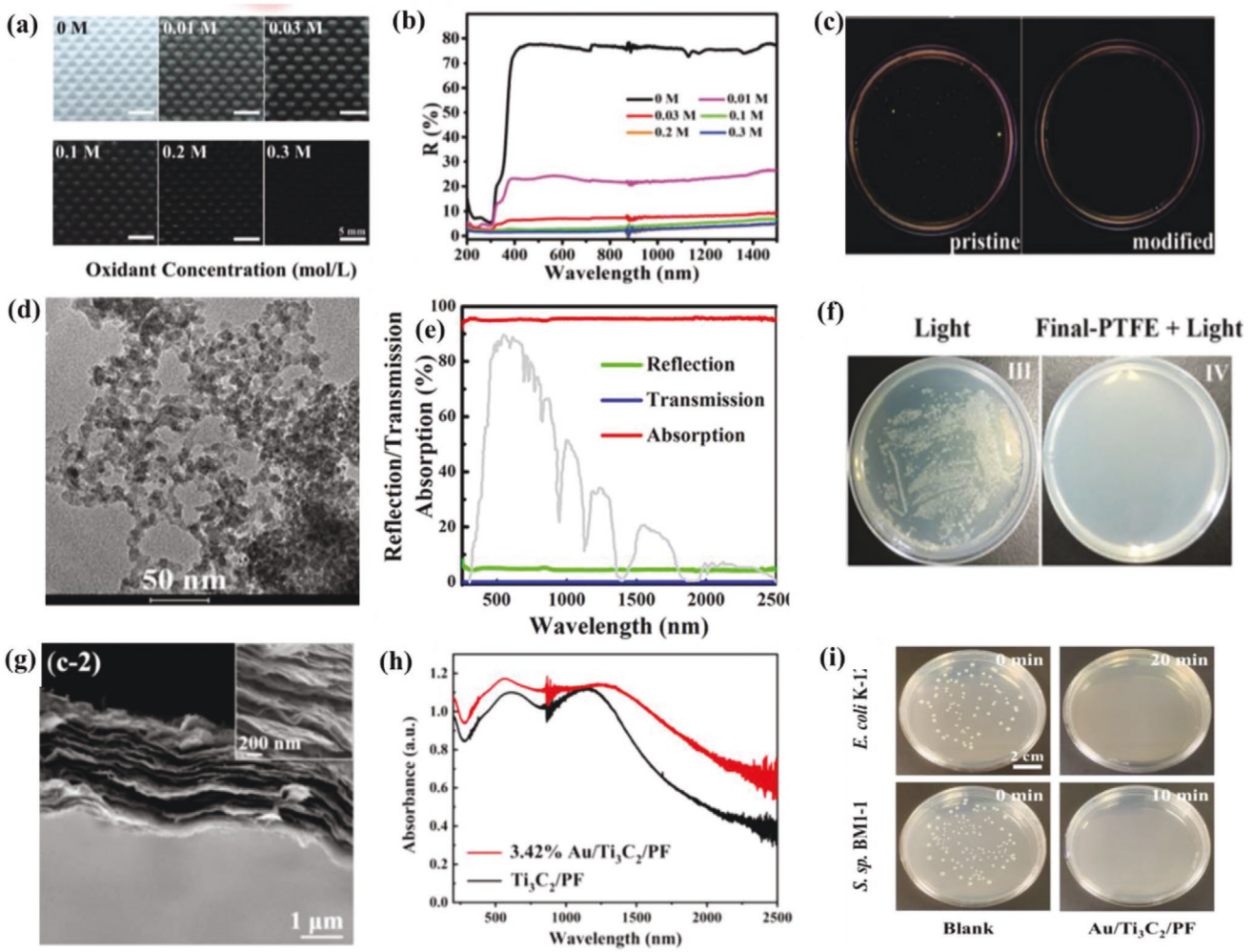

Figure 8. Photothermal bacterial killing. a) Optical images of different concentrations of polypyrrole-modified membranes. b) Their corresponding optical performances. c) Bacterial killing effect of pristine and polypyrrole-modified membranes. (a–c) Reproduced with permission.[120] Copyright 2019, The Royal Society of Chemistry. d) TEM image of $Co_{2.67}S_4$ nanoparticles. e) Optical properties of $Co_{2.67}S_4$ nanoparticles on PTFE substrate. f) Bacterial killing effects under different conditions. (d–f) Reproduced with permission. Copyright 2019, American Chemical Society. g) Cross section SEM images of 3.42% Au/Ti_3C_2/PF sample. h) Absorption spectrum of 3.42% Au/Ti_3C_2/PF and Ti_3C_2/PF samples. i) Bacterial killing effect of different kinds of germs under ≈2 Sun intensities. (g–i) Reproduced with permission.[41] Copyright 2021, American Chemical Society.

Sun, the device gained a high responsivity of 176.9 V W^{-1} with a long response-recovery time of about 80 s (Figure 9f). These findings will with no doubt expand the scope of applications of photothermal conversions of solar energy.

4.6. Photothermal Deicing

Freezing on the surface of objects sometimes will cause inconvenience and potential safety risks for daily life.[59,61,62] Therefore, it is necessary to develop new methods to address these issues. Compared with energy-consuming methods and environmentally unfriendly ones, photothermal deicing technology can make up for the above shortages, which only applies solar energy and photothermal materials. During the deicing process, the photothermal material absorbs the solar energy and causes a higher temperature surface, then the heat will be spontaneously delivered to the ice, causing its melt.

Photothermal deicing technology by solar energy is not only environmentally friendly and cost-effective, but also can solve a variety of safety hazards to our daily life, such as freezing car window will lead to poor eyesight, freezing stairs are easy to cause falling down, and so on. Wu et al.[61] demonstrated a candle soot-based hierarchical nanostructured photothermal material by placing a glass on the candle flame (**Figure 10**a) and some simple modifications (Figure 10b). When the sample with ice was placed under the solar light (Figure 10c), the light absorber (Figure 10c,d) absorbed the solar energy and converted it into heat. Then, the heat was delivered to the ice and led to its melt. Finally, the melted water rolled off the superhydrophobic surface. This self-clean photothermal material enables its high-efficiency deicing without contaminants under solar light. Susmita Dash and his coworkers[62] proposed a novel photothermal trap using solar energy for photothermal deicing. Their photothermal trap included three layers: insulation layer, heat spread layer, and light absorber. The achieved maximum

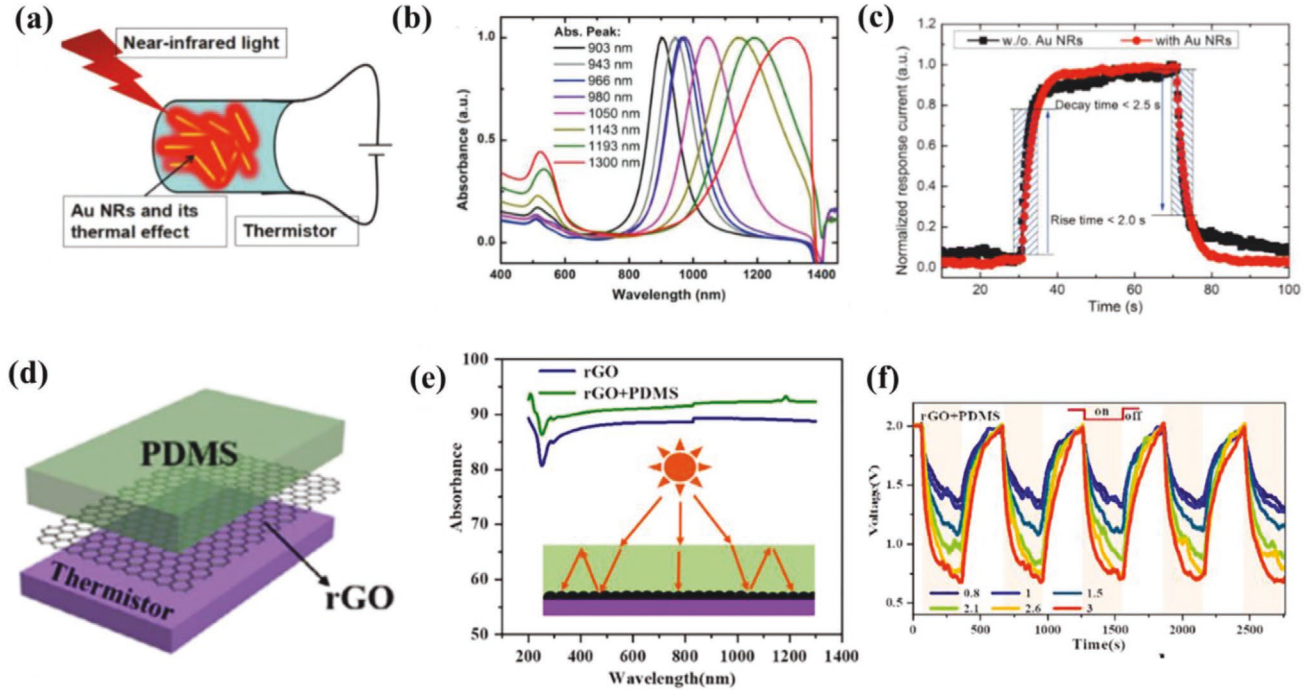

Figure 9. Photothermal sensors. a) Schematic illustration of Au-NR/thermistor device to harvest solar energy for sensing. b) Absorption spectrum of Au NRs in water. c) Normalized photo-responsive curves with/without Au NRs under the illumination of a 0.5 mW laser (λ = 1.5 μm). Applied bias is 1 V. (a–c) Reproduced with permission.[30] Copyright 2018, Wiley-VCH. d) Schematic illustration of the PDMS encapsulated rGO film structure. e) Absorption spectrum of rGO and rGO + PDMS. The inset is the possible light absorption mechanism. f) Photo-responsive curves of rGO/PDMS composite film under different solar intensities. (d–f) Reproduced with permission.[29] Copyright 2021, Elsevier.

surface temperature was used to evaluate the deicing efficiency under the solar illumination. To explore the practical application possibility of the photothermal trap, outdoor performance (Figure 10e) tests were conducted on a cold but sunny day (solar intensity is about 600 ± 100 W m^{-2}). Figure 10f is the time-dependent temperature curves of the photothermal trap (red line) and a reference of the aluminum surface. In the same time period, the photothermal trap had a higher surface temperature (37 °C) than the reference (11 °C). As a result, the ice on the photothermal trap was melted and slit off while the other kept the same as previous (inset in Figure 10f). Figure 10g is the real-time ice removal effect with the photothermal trap and the reference. Obviously, the ice on the photothermal trap can be totally removed with solar light after 5 min. The presented photothermal deicing surfaces exhibit significant impacts on solving potential risks in our daily life for the human community.

5. Conclusions and Outlook

For solar energy based on photothermal conversion, four fundamental principles (non-radiative relaxation of semiconductors, plasmonic heating of metallic nanostructures, thermal vibration of organic molecules, and multiple interactions of micro/nanostructured materials) and hybrid mechanisms of thermal releasing are summarized regarding on different types of photothermal materials. These photothermal materials should have excellent light trapping performance, suitable heat conduction, low emission, and high stability simultaneously, so that they can utilize solar energy as much as possible and have the potential to practical applications. The details of preparation methods, the thermal releasing type, broadband absorption range, and application fields of photothermal materials are summarized in **Table 1**. Most broadband photothermal materials have the unique advantages that enable them with strong light absorption in broadband range, that is, the whole solar spectrum and possess the excellent heat conduction performance that allow them to transfer heat to the thermally sensitive mediums, resulting in broad ranges of application prospects. In this review, we comprehensively summarized the state-of-the-art photothermal applications for solar energy conversion, including photothermal water evaporation and desalination, photothermal catalysis for H_2 generation and CO_2 reduction, photothermal electric power generation, photothermal bacterial killing, photothermal sensors, and photothermal deicing. These solar energy conversion technologies offer new opportunities for development of cost-effective, environmentally friendly, highly efficient, and sustainable photothermal converters that work only in sunlight and ambient conditions. While more efforts in both, fundamental research and practical applications, should be taken to further improve the performance, reduce the costs, and extend the usage lifetime of photothermal converters.

For instance, at first, the development and reasonable selection of novel materials with high broadband absorption, suitable heat conduction, and low emission as the light absorbers

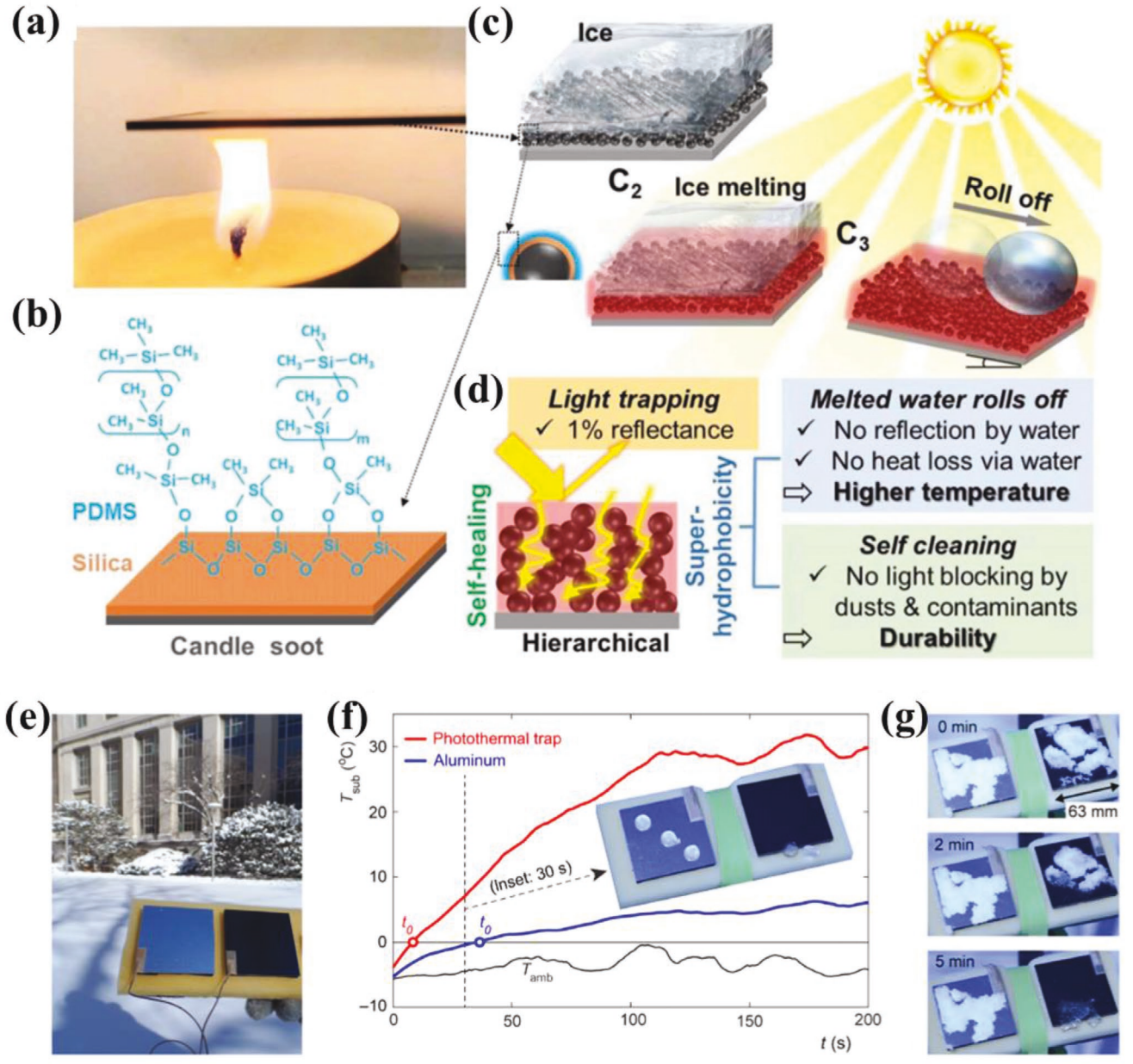

Figure 10. Photothermal deicing. a) Fabrication of candle soot absorber on a candle flame. b) Silica and PDMS coating on the candle soot surface. c) Deicing mechanism of superhydrophobic candle soot surface under the light illumination. d) High light trapping performance and superhydrophobicity enabled by the hierarchical structures. (a–d) Reproduced with permission.[61] Copyright 2020, National Academy of Sciences of the USA. e) Photothermal experiments outdoor. Aluminum surface (left) and photothermal trap (right). f) Temperature change curves for aluminum surface and photothermal trap under the solar intensity ≈0.6 Sun. g) Deicing comparison for aluminum surface and photothermal trap. (a–d) Reproduced with permission.[62] Copyright 2018, American Association for the Advancement of Science.

are critically significant for high photothermal conversion efficiency. A big challenge for high photothermal conversion efficiency is the lack of natural materials to allow for broadband absorption of solar energy. As a result, it is very difficult to achieve high solar conversion efficiency, which has been a barrier to the normal development of this area. Different strategies regarding on different thermal releasing mechanisms are proposed to improve the light trapping performance. For example, defect engineering including vacancies and doping can be adopted to produce defect energy level to enhance light absorption in semiconductor materials; metal nanoparticles with a strong LSPR effect can be attached to the special support with hierarchical structures to achieve a totally black surface; More π–π stacking should be introduced to cause more light absorption in organic materials; micro/nanostructured materials can extend the optical path length and thus increase the times of reflection and transmission with the structure, leading to strong absorption in a wide range; some other materials and hybrid

Table 1. The state-of-art literatures on the mechanisms, absorptance, and absorption ranges for different photothermal applications based on solar energy conversion.

Materials	Mechanisms[a)]	Absorptance	Absorption range [nm]	Photothermal applications[b)]	Ref.
$Ag/AgBr/CsPbBr_3$	M+S	~	300–1000	CH_4 reforming	[15]
Ni/TiO_2	M+S	~	200–1000	N_2 reduction	[16]
rGO/PDMS	C	92%	200–1300	photodetector	[29]
Al nanoparticles	M	~89%	400–2500	WE + desalination	[32]
Black silicon	S	98.9%	300–2500	Electric power	[34]
Au/Ti_3C_2	M+C	~	200–2500	WE + BK	[41]
$Cu_2O/g\text{-}C_3N_4$	S	~	–	CO_2 reduction	[42]
PPy	O	~	200–2000	photodetector	[43]
Ti_2O_3	S	~	300–1800	H_2	[44]
$H_{1.68}MoO_3$	S	>95	300–2500	WE + desalination	[45]
3D graphene	C	~97%	200–2500	WE + desalination	[47]
CuS	M	94%–95.5%	290–1400	WE	[48]
Au@silicon	M+S	~98%	200–1700	WE+ electric power	[51]
Black silver	M	99.5%	200–2500	WE	[52]
Black silicon	S	98.7%	300–2500	WE	[53]
Candle soot	C	~99%	–	deicing	[61]
Ni PCs	M	~95%	250–1500	WE	[89]
Liquid metals/polymer	M+O	96.9–99.3%	330–2100	Electric power	[90]
PU+CR	O	~95%	300–1600	WE	[92]
PP-PEDOT-PPy	O	~	–	Electric power	[93]
Pd-wood	M	>99%	250–2500	WE + desalination	[103]
Rh/Al	M	~	300–1200	CO_2 reduction	[110]
TiN–Pt	M	~	400–1000	H_2	[111]
Ni/SiO_2	M	~98%	200–2250	CO_2 reduction	[114]
PTC gel	S+M	>90%	250–2500	WE	[112]
Fe_3O_4/Fe_3C	S+C	~	200–2500	CO_2 reduction	[115]
$Si@Co@SiO_2$	S+M	98%	250–2500	CO_2 Reduction	[116]
PEDOT:PSS/Te	S+O	~	300–1100	Electric power	[118]
PPy	O	~95%	200–1500	BK	[120]
$Co_{2.67}S_4$-PTFE	S	~95%	250–2500	WE+BK	[121]
Wood/CoO	C+S	~75%	300–1000	H_2	[123]
Black TiO_2	S	~	250–2500	WE	[124]
HNb_3O_8/PAM	S+O	90%	250–2500	WE	[125]
TiN	M	~	300–1400	CO oxidation	[126]
Mxene-textil	C	~	–	BK	[127]
polymer porous foam (PPy)	O	90%	200–2500	WE	[128]
CS aerogel	C	~97%	250–2500	WE	[129]
Wood-PPy	C+O	>90%	300–2500	WE	[130]
$Pt/Au/TiO_2$	M+C+S	~	200–900	WE+PD	[131]
CNT/PEI/MCE	C	~	500–2500	WE+BK	[132]
Carbon sponge	C	~	–	WE+ electric power	[133]
Black bamboos	C	97%	250–2500	WE	[134]
Te nanoparticles	S	~90%	300–2000	WE	[135]
Co–Cu–Mn	M+S	~	–	CO_2 reduction	[136]
AlCrWTaNbTiN	M	~93%	0–11000	~	[137]

Table 1. Continued.

Materials	Mechanisms[a)]	Absorptance	Absorption range [nm]	Photothermal applications[b)]	Ref.
$Ni/CeO_2/SiO_2$	M+S	~	200–1000	CH_4 reforming	[138]
COF	O	~	–	Cycloaddition	[139]
Laser-induced Graphene	C	~85%	500–2000	Actuator	[140]
$Ti_3C_2T_x$ MXene	C	~	–	Actuator	[141]
$Au\text{-}Cu_{1.97}S/Cu_2S$	M	~	300–2500	photodetector	[142]
Mxene/Au	C+M	~	300–800	BK	[143]

[a)]S = non-radiative relaxation of semiconductors; M = plasmonic heating of metals; O = Thermal vibration of organic molecules; C = multiple interactions of micro/nano-structured materials; [b)]WE = water evaporation; BK = bacterial killing; PD = photodegradation.

materials can also combine two or three above mentioned strategies to boost solar light absorption. In addition, the suitable thermal conduction of photothermal materials is also of great significance for high solar conversion efficiency. In that case, the excellent light absorber will absorb solar light and the transferred heat can be as much as possible to be used for interfacial water evaporation and desalination, electric power generation, catalysis, bacterial killing, and sensors. It is also necessary for the light absorber with low heat emission to ensure high solar energy conversion efficiency.

Second, multi-level stability regarding on illumination, water, acid, salts, base, thermal, and bacteria are highly demanded for realistic photothermal operations. The robust stability of photothermal converters is also a large challenge when operating them in realistic circumstance, such as high concentration solar intensity, river water, seawater, acid, base, high temperature, and so on. Extensive attention has been paid to the maximum photothermal conversion efficiency, while very limited research was focused on the photothermal converter in real operation conditions. The usage lifetime of photothermal converters directly decides whether they can be used in reality or not and thus stability is quite important. More work should be conducted to study and improve the stability of their practical applications, such as studying the influence of surface chemistry on stability and developing anti-corrosion (light and chemistry corrosion) materials.

Third, the development of earth-abundant photothermal materials should be more focused to reduce the cost barrier for extensive commercial applications. Though noble metal nanoparticles with broadband light absorption can show excellent photothermal water evaporation, electric power generation, catalysis for chemical energy production, and bacterial killing performances, they are very rare on the earth and costly, which can be the biggest obstacle to the practical commercial applications. Alternatively, some light absorbers have also been developed with nanoparticles of earth-abundant metal elements, such as Fe, Ni, and Al, and demonstrated promising solar energy harvesting performance. Therefore, more attention should be paid to these cost-effective elements

Furthermore, fabrication technologies with large-scale, controllable parameters and low cost are also highly needed to be applied for promoting the realistic application. It can be expected that the further development and commercialization of the diverse photothermal technologies for solar energy conversion will play an important role and have big significance on global sustainability.

Acknowledgements

This work was supported by Deutsche Forschungsgemeinschaft (DFG Grant Scha 632/24, within SPP1839 "Tailored Disorder"). Additionally, P.C. was supported by a China Scholarship Council (CSC) fellowship. Support by the Center of Micro- and Nanotechnologies (ZMN), a DFG-funded core facility of TU Ilmenau, is gratefully acknowledged.

Open access funding enabled and organized by Projekt DEAL.

Conflict of Interest

The authors declare no conflict of interest.

Keywords

broadband light absorbers, photothermal applications, photothermal mechanisms, solar energy conversion, sustainable energy technologies

Received: March 9, 2022
Revised: June 20, 2022
Published online: July 6, 2022

[1] J. M. Chen, *Innovation* **2021**, *2*, 100127.
[2] A. Grainger, G. Smith, *Curr. Opin. Environ. Sustainability* **2021**, *49*, 164.
[3] M. K. H. Rabaia, M. A. Abdelkareem, E. T. Sayed, K. Elsaid, K.-J. Chae, T. Wilberforce, A. G. Olabi, *Sci. Total Environ.* **2021**, *754*, 141989.
[4] L. Kruitwagen, K. T. Story, J. Friedrich, L. Byers, S. Skillman, C. Hepburn, *Nature* **2021**, *598*, 604.
[5] L. Jin, H. Zhao, Z. M. Wang, F. Rosei, *Adv. Energy Mater.* **2021**, *11*, 2003233.
[6] S. Gorjian, H. Sharon, H. Ebadi, K. Kant, F. B. Scavo, G. M. Tina, *J. Cleaner Prod.* **2021**, *278*, 124285.
[7] C. Liu, D. Kong, P.-C. Hsu, H. Yuan, H.-W. Lee, Y. Liu, H. Wang, S. Wang, K. Yan, D. Lin, P. A. Maraccini, K. M. Parker, A. B. Boehm, Y. Cui, *Nat. Nanotechnol.* **2016**, *11*, 1098.
[8] J. Gong, C. Li, M. R. Wasielewski, *Chem. Soc. Rev.* **2019**, *48*, 1862.
[9] H. Yeom, K. Sridharan, *Ann. Nucl. Energy* **2021**, *150*, 107835.
[10] K. Johansen, *Energy Policy* **2021**, *152*, 112139.
[11] C. Zhang, L. Zhou, P. Cheng, D. Liu, C. Zhang, X. Li, S. Li, J. Wang, Z. L. Wang, *Adv. Energy Mater.* **2021**, *11*, 2003616.
[12] R. Peibst, M. Rienäcker, Y. Larionova, N. Folchert, F. Haase, C. Hollemann, S. Wolter, J. Krügener, P. Bayerl, J. Bayer, M. Dzinnik, R. J. Haug, R. Brendel, *Sol. Energy Mater. Sol. Cells* **2022**, *238*, 111560.

[13] L. Lin, T. W. Jones, T. C.-J. Yang, N. W. Duffy, J. Li, L. Zhao, B. Chi, X. Wang, G. J. Wilson, *Adv. Funct. Mater.* **2021**, *31*, 2008300.
[14] A. Al-Ashouri, E. Köhnen, B. Li, A. Magomedov, H. Hempel, P. Caprioglio, J. A. Márquez, A. B. M. Vilches, E. Kasparavicius, J. A. Smith, N. Phung, D. Menzel, M. Grischek, L. Kegelmann, D. Skroblin, C. Gollwitzer, T. Malinauskas, M. Jošt, G. Matič, B. Rech, R. Schlatmann, M. Topič, L. Korte, A. Abate, B. Stannowski, D. Neher, M. Stolterfoht, T. Unold, V. Getautis, S. Albrecht, *Science* **2020**, *370*, 1300.
[15] P. Gao, P. Wang, X. Liu, Z. Cui, Y. Wu, X. Zhang, Q. Zhang, Z. Wang, Z. Zheng, H. Cheng, Y. Liu, Y. Dai, B. Huang, *Catal. Sci. Technol.* **2022**, *12*, 1628.
[16] S. Wang, W. Yu, S. Xu, K. Han, F. Wang, *ACS Sustainable Chem. Eng.* **2022**, *10*, 115.
[17] D. Mateo, J. L. Cerrillo, S. Durini, J. Gascon, *Chem. Soc. Rev.* **2021**, *50*, 2173.
[18] M. Ghoussoub, M. Xia, P. N. Duchesne, D. Segal, G. Ozin, *Energy Environ. Sci.* **2019**, *12*, 1122.
[19] W. K. Fan, M. Tahir, *Chem. Eng. J.* **2022**, *427*, 131617.
[20] L. Zhu, M. Gao, C. K. N. Peh, G. W. Ho, *Nano Energy* **2019**, *57*, 507.
[21] H. Ren, M. Tang, B. Guan, K. Wang, J. Yang, F. Wang, M. Wang, J. Shan, Z. Chen, D. Wei, H. Peng, Z. Liu, *Adv. Mater.* **2017**, *29*, 1702590.
[22] Q. Chen, Z. Pei, Y. Xu, Z. Li, Y. Yang, Y. Wei, Y. Ji, *Chem. Sci.* **2018**, *9*, 623.
[23] Y. Shi, R. Li, Y. Jin, S. Zhuo, L. Shi, J. Chang, S. Hong, K.-C. Ng, P. Wang, *Joule* **2018**, *2*, 1171.
[24] M. Gao, L. Zhu, C. Kangnuo Peh, G. Wei Ho, *Energy Environ. Sci.* **2019**, *12*, 841.
[25] C. Zhang, H.-Q. Liang, Z.-K. Xu, Z. Wang, *Adv. Sci.* **2019**, *6*, 1900883.
[26] F. Zhao, Y. Guo, X. Zhou, W. Shi, G. Yu, *Nat. Rev. Mater.* **2020**, *5*, 388.
[27] P. Tao, G. Ni, C. Song, W. Shang, J. Wu, J. Zhu, G. Chen, T. Deng, *Nat. Energy* **2018**, *3*, 1031.
[28] Y. Zou, Y. Zhang, Q. Yu, H. Chen, *Biomater. Sci.* **2021**, *9*, 10.
[29] M. Xiong, X. Shan, C. Liu, L. Yang, M. Meng, Y. Di, Z. Gan, *Appl. Surf. Sci. Adv.* **2021**, *3*, 100050.
[30] H. Xiang, T. Niu, M. Schoenauer Sebag, Z. Hu, X. Xu, L. Billot, L. Aigouy, Z. Chen, *Small* **2018**, *14*, 1704013.
[31] B. Han, Y.-L. Zhang, Q.-D. Chen, H.-B. Sun, *Adv. Funct. Mater.* **2018**, *28*, 1802235.
[32] L. Zhou, Y. Tan, J. Wang, W. Xu, Y. Yuan, W. Cai, S. Zhu, J. Zhu, *Nat. Photonics* **2016**, *10*, 393.
[33] C. Chen, Y. Kuang, L. Hu, *Joule* **2019**, *3*, 683.
[34] P. Cheng, H. Wang, B. Müller, J. Müller, D. Wang, P. Schaaf, *ACS Appl. Mater. Interfaces* **2021**, *13*, 1818.
[35] Z. Wu, C. Li, Z. Li, K. Feng, M. Cai, D. Zhang, S. Wang, M. Chu, C. Zhang, J. Shen, Z. Huang, Y. Xiao, G. A. Ozin, X. Zhang, L. He, *ACS Nano* **2021**, *15*, 5696.
[36] S. Luo, X. Ren, H. Lin, H. Song, J. Ye, *Chem. Sci.* **2021**, *12*, 5701.
[37] C. Yao, Q. Wang, Y. Lin, W. Jin, L. Xiao, S. Gao, Y. Wang, P. Wang, W. Ren, *Opt. Lett.* **2019**, *44*, 4048.
[38] D. Zhang, Y. Song, L. Ping, S. Xu, D. Yang, Y. Wang, Y. Yang, *Nano Res.* **2019**, *12*, 2982.
[39] L. Zhu, T. Ding, M. Gao, C. K. N. Peh, G. W. Ho, *Adv. Energy Mater.* **2019**, *9*, 1900250.
[40] K. Vikrant, S. Weon, K.-H. Kim, M. Sillanpää, *Appl. Mater. Today* **2021**, *23*, 100993.
[41] W. Qu, H. Zhao, Q. Zhang, D. Xia, Z. Tang, Q. Chen, C. He, D. Shu, *ACS Sustainable Chem. Eng.* **2021**, *9*, 11372.
[42] P. Li, L. Liu, W. An, H. Wang, W. Cui, *Appl. Surf. Sci.* **2021**, *565*, 150448.
[43] H. Xiang, C. Xin, Z. Hu, L. Aigouy, Z. Chen, X. Yuan, *ACS Appl. Mater. Interfaces* **2021**, *13*, 45957.
[44] H. Huang, C. Wang, Q. Li, R. Wang, Y. Yang, A. Muhetaer, F. Huang, B. Han, D. Xu, *Adv. Funct. Mater.* **2021**, *31*, 2007591.
[45] Q. Zhu, K. Ye, W. Zhu, W. Xu, C. Zou, L. Song, E. Sharman, L. Wang, S. Jin, G. Zhang, Y. Luo, J. Jiang, *J. Phys. Chem. Lett.* **2020**, *11*, 2502.
[46] Y. Zhou, T. Ding, M. Gao, K. H. Chan, Y. Cheng, J. He, G. W. Ho, *Nano Energy* **2020**, *77*, 105102.
[47] Y. Yang, R. Zhao, T. Zhang, K. Zhao, P. Xiao, Y. Ma, P. M. Ajayan, G. Shi, Y. Chen, *ACS Nano* **2018**, *12*, 829.
[48] X. Wu, M. E. Robson, J. L. Phelps, J. S. Tan, B. Shao, G. Owens, H. Xu, *Nano Energy* **2019**, *56*, 708.
[49] G. Liu, J. Xu, K. Wang, *Nano Energy* **2017**, *41*, 269.
[50] J. Wang, Y. Li, L. Deng, N. Wei, Y. Weng, S. Dong, D. Qi, J. Qiu, X. Chen, T. Wu, *Adv. Mater.* **2017**, *29*, 1603730.
[51] Z. Zhang, Y. Wang, P. A. Stensby Hansen, K. Du, K. R. Gustavsen, G. Liu, F. Karlsen, O. Nilsen, C. Xue, K. Wang, *Nano Energy* **2019**, *65*, 103992.
[52] P. Cheng, M. Ziegler, V. Ripka, D. Wang, H. Wang, P. A. van Aken, P. Schaaf, *Appl. Mater. Today* **2021**, *25*, 101238.
[53] P. Cheng, H. Wang, H. Wang, P. A. van Aken, D. Wang, P. Schaaf, *Adv. Energy Sustainable Res.* **2021**, *2*, 2000083.
[54] D. Kraemer, Q. Jie, K. McEnaney, F. Cao, W. Liu, L. A. Weinstein, J. Loomis, Z. Ren, G. Chen, *Nat. Energy* **2016**, *1*, 16153.
[55] Y. Peng, W. Zhao, F. Ni, W. Yu, X. Liu, *ACS Nano* **2021**, *15*, 19490.
[56] R. Liu, J. Li, J. Duan, B. Yu, W. Xie, B. Qi, H. Wang, X. Zhuang, S. Liu, P. Liu, G. Tao, M. Xu, J. Zhou, *Cell Rep. Phys. Sci.* **2021**, *2*, 100533.
[57] J. Tian, L. Chen, R. Qiao, K. Xiong, W. Zhang, Y. Mao, H. Li, J. Li, *Nano Energy* **2021**, *79*, 105435.
[58] Z. Xie, H. Wang, Y. Geng, M. Li, Q. Deng, Y. Tian, R. Chen, X. Zhu, Q. Liao, *ACS Appl. Mater. Interfaces* **2021**, *13*, 48308.
[59] W. Zheng, L. Teng, Y. Lai, T. Zhu, S. Li, X. Wu, W. Cai, Z. Chen, J. Huang, *Chem. Eng. J.* **2022**, *427*, 130922.
[60] T. Hao, Z. Zhu, H. Yang, Z. He, J. Wang, *ACS Appl. Mater. Interfaces* **2021**, *13*, 44948.
[61] S. Wu, Y. Du, Y. Alsaid, D. Wu, M. Hua, Y. Yan, B. Yao, Y. Ma, X. Zhu, X. He, *Proc. Natl. Acad. Sci. USA* **2020**, *117*, 11240.
[62] S. Dash, J. de Ruiter, K. K. Varanasi, *Sci. Adv.* **2018**, *4*, eaat0127.
[63] M. Li, N. Han, X. Zhang, S. Wang, M. Jiang, A. Bokhari, W. Zhang, M. Race, Z. Shen, R. Chen, M. Mubashir, K. S. Khoo, S. S. Teo, P. L. Show, *Environ. Res.* **2022**, *205*, 112544.
[64] X. Che, B. Zhu, P. Wang, *Energy Policy* **2021**, *149*, 112099.
[65] H. Min, D. Y. Lee, J. Kim, G. Kim, K. S. Lee, J. Kim, M. J. Paik, Y. K. Kim, K. S. Kim, M. G. Kim, T. J. Shin, S. Il Seok, *Nature* **2021**, *598*, 444.
[66] S. Chen, X. Dai, S. Xu, H. Jiao, L. Zhao, J. Huang, *Science* **2021**, *373*, 902.
[67] J. J. Yoo, G. Seo, M. R. Chua, T. G. Park, Y. Lu, F. Rotermund, Y.-K. Kim, C. S. Moon, N. J. Jeon, J.-P. Correa-Baena, V. Bulović, S. S. Shin, M. G. Bawendi, J. Seo, *Nature* **2021**, *590*, 587.
[68] M. W. Campbell, V. C. Polites, S. Patel, J. E. Lipson, J. Majhi, G. A. Molander, *J. Am. Chem. Soc.* **2021**, *143*, 19648.
[69] M. J. Genzink, J. B. Kidd, W. B. Swords, T. P. Yoon, *Chem. Rev.* **2022**, *122*, 1654.
[70] R. Kusaka, S. Nihonyanagi, T. Tahara, *Nat. Chem.* **2021**, *13*, 306.
[71] Z. Mei, Y. Chen, S. Tong, Y. Li, J. Liu, L. Sun, W. Zhong, X. Dong, Y. Ji, Y. Lin, H. Chen, F. Pan, *Adv. Funct. Mater.* **2022**, *32*, 2107164.
[72] R. Tang, S. Zhou, Z. Zhang, R. Zheng, J. Huang, *Adv. Mater.* **2021**, *33*, 2005389.
[73] X. Zhang, P. Zhai, Y. Zhang, Y. Wu, C. Wang, L. Ran, J. Gao, Z. Li, B. Zhang, Z. Fan, L. Sun, J. Hou, *J. Am. Chem. Soc.* **2021**, *143*, 20657.
[74] D. Xu, Z. Li, L. Li, J. Wang, *Adv. Funct. Mater.* **2020**, *30*, 2000712.
[75] L. Zhu, M. Gao, C. K. Nuo Peh, G. W. Ho, *Mater. Horiz.* **2018**, *5*, 323.

[76] J. Pan, X. Yu, J. Dong, L. Zhao, L. Liu, J. Liu, X. Zhao, L. Liu, *ACS Appl. Mater. Interfaces* **2021**, *13*, 58124.
[77] Y. Yan, B. Hao, D. Wang, G. Chen, E. Markweg, A. Albrecht, P. Schaaf, *J. Mater. Chem. A* **2013**, *1*, 14507.
[78] Y. Yan, M. Han, A. Konkin, T. Koppe, D. Wang, T. Andreu, G. Chen, U. Vetter, J. Ramón Morante, P. Schaaf, *J. Mater. Chem. A* **2014**, *2*, 12708.
[79] W. Ren, Y. Yan, L. Zeng, Z. Shi, A. Gong, P. Schaaf, D. Wang, J. Zhao, B. Zou, H. Yu, G. Chen, E. M. B. Brown, A. Wu, *Adv. Healthcare Mater.* **2015**, *4*, 1526.
[80] Y. Cai, H. Zhu, Q. Shi, Y. Cheng, L. Chang, W. Huang, *iScience* **2022**, *25*, 103661.
[81] Y. Xiao, K. Wang, Z. Yang, Z. Xing, Z. Li, K. Pan, W. Zhou, *J. Hazard. Mater.* **2021**, *414*, 125487.
[82] K. Nabeela, M. N. Thorat, S. N. Backer, A. M. Ramachandran, R. T. Thomas, G. Preethikumar, A. P. Mohamed, A. Asok, S. G. Dastager, S. Pillai, *ACS Appl. Bio Mater.* **2021**, *4*, 4373.
[83] S. Linic, U. Aslam, C. Boerigter, M. Morabito, *Nat. Mater.* **2015**, *14*, 567.
[84] X.-M. Li, M.-H. Bi, L. Cui, Y.-Z. Zhou, X.-W. Du, S.-Z. Qiao, J. Yang, *Adv. Funct. Mater.* **2017**, *27*, 1605703.
[85] L. Wang, M. Hasanzadeh Kafshgari, M. Meunier, *Adv. Funct. Mater.* **2020**, *30*, 2005400.
[86] K. L. Kelly, E. Coronado, L. L. Zhao, G. C. Schatz, *J. Phys. Chem. B* **2003**, *107*, 668.
[87] P. K. Jain, X. Huang, I. H. El-Sayed, M. A. El-Sayed, *Acc. Chem. Res.* **2008**, *41*, 1578.
[88] L. Zhou, Y. Tan, D. Ji, B. Zhu, P. Zhang, J. Xu, Q. Gan, Z. Yu, J. Zhu, *Sci. Adv.* **2016**, *2*, e1501227.
[89] R. Xu, H. Zhao, H. Jin, Z. Wang, Z. Zhang, S. Xu, Z. Zeng, S. Wang, Y. Lei, *Nano Energy* **2019**, *58*, 543.
[90] X. Huang, J. Liu, P. Zhou, G. Su, T. Zhou, X. Zhang, C. Zhang, *Small* **2022**, *18*, 2104048.
[91] Y. Zhang, G. G. Gurzadyan, M. M. Umair, W. Wang, R. Lu, S. Zhang, B. Tang, *Chem. Eng. J.* **2018**, *344*, 402.
[92] G. Chen, J. Sun, Q. Peng, Q. Sun, G. Wang, Y. Cai, X. Gu, Z. Shuai, B. Z. Tang, *Adv. Mater.* **2020**, *32*, 1908537.
[93] X. Zhang, T.-T. Li, H.-T. Ren, H.-K. Peng, B.-C. Shiu, Y. Wang, C.-W. Lou, J.-H. Lin, *ACS Appl. Mater. Interfaces* **2020**, *12*, 55072.
[94] G. Chen, Z. Jiang, A. Li, X. Chen, Z. Ma, H. Song, *J. Mater. Chem. A* **2021**, *9*, 16805.
[95] P. Cao, L. Zhao, J. Zhang, L. Zhang, P. Yuan, Y. Zhang, Q. Li, *ACS Appl. Mater. Interfaces* **2021**, *13*, 19109.
[96] Y. Duan, M. Weng, W. Zhang, Y. Qian, Z. Luo, L. Chen, *Energy Convers. Manag.* **2021**, *241*, 114306.
[97] W. He, L. Zhou, M. Wang, Y. Cao, X. Chen, X. Hou, *Sci. Bull.* **2021**, *66*, 1472.
[98] P. Lova, V. Robbiano, F. Cacialli, D. Comoretto, C. Soci, *ACS Appl. Mater. Interfaces* **2018**, *10*, 33434.
[99] P. Cheng, M. Ziegler, V. Ripka, H. Wang, K. Pollok, F. Langenhorst, D. Wang, P. Schaaf, *ACS Appl. Mater. Interfaces* **2022**, *14*, 16894.
[100] R. Li, L. Zhang, L. Shi, P. Wang, *ACS Nano* **2017**, *11*, 3752.
[101] Z. Liu, Z. Zhou, N. Wu, R. Zhang, B. Zhu, H. Jin, Y. Zhang, M. Zhu, Z. Chen, *ACS Nano* **2021**, *15*, 13007.
[102] S. Dong, Y. Zhao, J. Yang, X. Liu, W. Li, L. Zhang, Y. Wu, J. Sun, J. Feng, Y. Zhu, *Appl. Catal., B* **2021**, *291*, 120127.
[103] M. Zhu, Y. Li, F. Chen, X. Zhu, J. Dai, Y. Li, Z. Yang, X. Yan, J. Song, Y. Wang, E. Hitz, W. Luo, M. Lu, B. Yang, L. Hu, *Adv. Energy Mater.* **2018**, *8*, 1701028.
[104] S. Hu, J. Shi, B. Luo, C. Ai, D. Jing, *J. Colloid Interface Sci.* **2022**, *608*, 2058.
[105] F. Yu, C. Wang, Y. Li, H. Ma, R. Wang, Y. Liu, N. Suzuki, C. Terashima, B. Ohtani, T. Ochiai, A. Fujishima, X. Zhang, *Adv. Sci.* **2020**, *7*, 2000204.
[106] Z. Wang, H. Song, H. Liu, J. Ye, *Angew. Chem., Int. Ed.* **2020**, *59*, 8016.
[107] S. Fang, Y. H. Hu, *Chem. Soc. Rev.* **2022**, *51*, 3609.
[108] J. Hong, C. Xu, B. Deng, Y. Gao, X. Zhu, X. Zhang, Y. Zhang, *Adv. Sci.* **2022**, *9*, 2103926.
[109] Y. Zhao, W. Gao, S. Li, G. R. Williams, A. H. Mahadi, D. Ma, *Joule* **2019**, *3*, 920.
[110] G. Fu, M. Jiang, J. Liu, K. Zhang, Y. Hu, Y. Xiong, A. Tao, Z. Tie, Z. Jin, *Nano Lett.* **2021**, *21*, 8824.
[111] S. Rej, L. Mascaretti, E. Y. Santiago, O. Tomanec, Š. Kment, Z. Wang, R. Zbořil, P. Fornasiero, A. O. Govorov, A. Naldoni, *ACS Catal.* **2020**, *10*, 5261.
[112] M. Gao, C. K. Peh, L. Zhu, G. Yilmaz, G. W. Ho, *Adv. Energy Mater.* **2020**, *10*, 2000925.
[113] Q. Wang, X. Cheng, Y. Sun, Z. Sun, D. Wang, G. Chen, P. Schaaf, *Mater. Adv.* **2021**, *2*, 2104.
[114] M. Cai, Z. Wu, Z. Li, L. Wang, W. Sun, A. A. Tountas, C. Li, S. Wang, K. Feng, A.-B. Xu, S. Tang, A. Tavasoli, M. Peng, W. Liu, A. S. Helmy, L. He, G. A. Ozin, X. Zhang, *Nat. Energy* **2021**, *6*, 807.
[115] C. Song, X. Liu, M. Xu, D. Masi, Y. Wang, Y. Deng, M. Zhang, X. Qin, K. Feng, J. Yan, J. Leng, Z. Wang, Y. Xu, B. Yan, S. Jin, D. Xu, Z. Yin, D. Xiao, D. Ma, *ACS Catal.* **2020**, *10*, 10364.
[116] D. Zhang, K. Lv, C. Li, Y. Fang, S. Wang, Z. Chen, Z. Wu, W. Guan, D. Lou, W. Sun, D. Yang, L. He, X. Zhang, *Sol. RRL* **2021**, *5*, 2000387.
[117] H. Zhang, W. Cheng, D. Luan, X. W. (David) Lou, *Angew. Chem., Int. Ed.* **2021**, *60*, 13177.
[118] Y. Liu, X. Lan, J. Xu, W. Zhou, C. Liu, C. Liu, P. Liu, M. Li, F. Jiang, *ACS Appl. Mater. Interfaces* **2021**, *13*, 43155.
[119] P. Cheng, Q. Zhou, X. Hu, S. Su, X. Wang, M. Jin, L. Shui, X. Gao, Y. Guan, R. Nözel, G. Zhou, Z. Zhang, J. Liu, *ACS Appl. Mater. Interfaces* **2018**, *10*, 23444.
[120] Q. Pan, S. Zhang, R. Li, Y. He, Y. Wang, *J. Mater. Chem. B* **2019**, *7*, 2948.
[121] L. Zhao, Q. Yang, W. Guo, H. Liu, T. Ma, F. Qu, *ACS Appl. Mater. Interfaces* **2019**, *11*, 20820.
[122] S. Tu, L. Xu, J. K. El-Demellawi, H. Liang, X. Xu, S. Lopatin, S. De Wolf, X. Zhang, H. N. Alshareef, *Nano Energy* **2020**, *77*, 105277.
[123] S. Guo, X. Li, J. Li, B. Wei, *Nat. Commun.* **2021**, *12*, 1343.
[124] I. Zada, W. Zhang, P. Sun, M. Imtiaz, N. Iqbal, U. Ghani, R. Naz, Y. Zhang, Y. Li, J. Gu, Q. Liu, D. Pantelić, B. Jelenković, D. Zhang, *Appl. Mater. Today* **2020**, *20*, 100669.
[125] M.-Q. Yang, C. F. Tan, W. Lu, K. Zeng, G. W. Ho, *Adv. Funct. Mater.* **2020**, *30*, 2004460.
[126] A. Naldoni, Z. A. Kudyshev, L. Mascaretti, S. P. Sarmah, S. Rej, J. P. Froning, O. Tomanec, J. E. Yoo, D. Wang, Š. Kment, T. Montini, P. Fornasiero, V. M. Shalaev, P. Schmuki, A. Boltasseva, R. Zbořil, *Nano Lett.* **2020**, *20*, 3663.
[127] X. Liu, X. Jin, L. Li, J. Wang, Y. Yang, Y. Cao, W. Wang, *J. Mater. Chem. A* **2020**, *8*, 12526.
[128] J. He, Z. Zhang, C. Xiao, F. Liu, H. Sun, Z. Zhu, W. Liang, A. Li, *ACS Appl. Mater. Interfaces* **2020**, *12*, 16308.
[129] Y. Gu, X. Mu, P. Wang, X. Wang, J. Liu, J. Shi, A. Wei, Y. Tian, G. Zhu, H. Xu, J. Zhou, L. Miao, *Nano Energy* **2020**, *74*, 104857.
[130] Z. Wang, Y. Yan, X. Shen, C. Jin, Q. Sun, H. Li, *J. Mater. Chem. A* **2019**, *7*, 20706.
[131] M. Wang, P. Wang, J. Zhang, C. Li, Y. Jin, *ChemSusChem* **2019**, *12*, 467.
[132] Y. Li, X. Cui, M. Zhao, Y. Xu, L. Chen, Z. Cao, S. Yang, Y. Wang, *J. Mater. Chem. A* **2019**, *7*, 704.
[133] L. Zhu, M. Gao, C. K. N. Peh, X. Wang, G. W. Ho, *Adv. Energy Mater.* **2018**, *8*, 1702149.
[134] J. Liu, J. Yao, Y. Yuan, Q. Liu, W. Zhang, X. Zhang, J. Gu, *Adv. Sustainable Syst.* **2020**, *4*, 2000126.
[135] C. Ma, J. Yan, Y. Huang, C. Wang, G. Yang, *Sci. Adv.* **2018**, *4*, eaas9894.
[136] Z.-H. He, Z.-H. Li, Z.-Y. Wang, K. Wang, Y.-C. Sun, S.-W. Wang, W.-T. Wang, Y. Yang, Z.-T. Liu, *Green Chem.* **2021**, *23*, 5775.
[137] C.-Y. He, X.-H. Gao, X.-L. Qiu, D.-M. Yu, H.-X. Guo, G. Liu, *Sol. RRL* **2021**, *5*, 2000790.

[138] K. Han, Y. Wang, S. Wang, Q. Liu, Z. Deng, F. Wang, *Chem. Eng. J.* **2021**, *421*, 129989.
[139] L.-G. Ding, B.-J. Yao, W.-X. Wu, Z.-G. Yu, X.-Y. Wang, J.-L. Kan, Y.-B. Dong, *Inorg. Chem.* **2021**, *60*, 12591.
[140] W. Wang, B. Han, Y. Zhang, Q. Li, Y.-L. Zhang, D.-D. Han, H.-B. Sun, *Adv. Funct. Mater.* **2021**, *31*, 2006179.
[141] Y. Hu, L. Yang, Q. Yan, Q. Ji, L. Chang, C. Zhang, J. Yan, R. Wang, L. Zhang, G. Wu, J. Sun, B. Zi, W. Chen, Y. Wu, *ACS Nano* **2021**, *15*, 5294.
[142] J. Tian, R. Qiao, K. Xiong, W. Zhang, L. Chen, *iScience* **2021**, *24*, 102167.
[143] Z. Yu, L. Jiang, R. Liu, W. Zhao, Z. Yang, J. Zhang, S. Jin, *Chem. Eng. J.* **2021**, *426*, 131914.

Pengfei Cheng received his B.S. degree from School of Materials Science and Engineering, Hubei University in 2015 and his M.Sc. degree from the South China Advanced Optoelectronic Academy, South China Normal University in 2019. Now, he is pursuing his Ph.D. degree at the Technische Universität Ilmenau under the supervision of Prof. Peter Schaaf and Dr. Dong Wang. His research interests focus on preparing nanostructured materials and their applications related with energy conversion.

Dong Wang studied Chemical Engineering at TU Wuhan for his B.Sc., and Materials Science at RWTH Aachen University for his M.Sc. He obtained his Ph.D. from Karlsruhe Institute of Technology in 2007. He conducted his 2 years postdoc research at Hannover University, and then has moved to TU Ilmenau. In 2016, he finished the Habilitation at TU Ilmenau, and currently is working as privatdozent there. His research interest is focused on tailored nanostructures and nanomaterials for photonic and energy applications.

Peter Schaaf studied Materials Physics at Saarland University and obtained his Diploma degree there in 1988. This is followed by earning his Ph.D. in 1991 with honors at the same university. After that, he moved to Göttingen University for a postdoc position in 1992. In 1995, he got an assistant professorship and was promoted to associate professor there in 1999. Since 2008, he is full professor at TU Ilmenau. His research interests lie in nanomaterials, electronic materials, nanotechnologies, thin films, functional materials, and materials analysis.